MODULE 1

1 Introduction

One picture is worth more than ten thousand words.

Anonymous

Preview

Interest in digital image processing methods stems from two principal application areas: improvement of pictorial information for human interpretation; and processing of image data for storage, transmission, and representation for autonomous machine perception. This chapter has several objectives: (1) to define the scope of the field that we call image processing; (2) to give a historical perspective of the origins of this field; (3) to give you an idea of the state of the art in image processing by examining some of the principal areas in which it is applied; (4) to discuss briefly the principal approaches used in digital image processing; (5) to give an overview of the components contained in a typical, general-purpose image processing system; and (6) to provide direction to the books and other literature where image processing work normally is reported.

1.1 What Is Digital Image Processing?

An image may be defined as a two-dimensional function, $f(x, y)$, where x and y are *spatial* (plane) coordinates, and the amplitude of f at any pair of coordinates (x, y) is called the *intensity* or *gray level* of the image at that point. When x, y, and the intensity values of f are all finite, discrete quantities, we call the image a *digital image*. The field of *digital image processing* refers to processing digital images by means of a digital computer. Note that a digital image is composed of a finite number of elements, each of which has a particular location

and value. These elements are called *picture elements*, *image elements*, *pels*, and *pixels*. *Pixel* is the term used most widely to denote the elements of a digital image. We consider these definitions in more formal terms in Chapter 2.

Vision is the most advanced of our senses, so it is not surprising that images play the single most important role in human perception. However, unlike humans, who are limited to the visual band of the electromagnetic (EM) spectrum, imaging machines cover almost the entire EM spectrum, ranging from gamma to radio waves. They can operate on images generated by sources that humans are not accustomed to associating with images. These include ultrasound, electron microscopy, and computer-generated images. Thus, digital image processing encompasses a wide and varied field of applications.

There is no general agreement among authors regarding where image processing stops and other related areas, such as image analysis and computer vision, start. Sometimes a distinction is made by defining image processing as a discipline in which both the input and output of a process are images. We believe this to be a limiting and somewhat artificial boundary. For example, under this definition, even the trivial task of computing the average intensity of an image (which yields a single number) would not be considered an image processing operation. On the other hand, there are fields such as computer vision whose ultimate goal is to use computers to emulate human vision, including learning and being able to make inferences and take actions based on visual inputs. This area itself is a branch of artificial intelligence (AI) whose objective is to emulate human intelligence. The field of AI is in its earliest stages of infancy in terms of development, with progress having been much slower than originally anticipated. The area of image analysis (also called image understanding) is in between image processing and computer vision.

There are no clear-cut boundaries in the continuum from image processing at one end to computer vision at the other. However, one useful paradigm is to consider three types of computerized processes in this continuum: low-, mid-, and high-level processes. Low-level processes involve primitive operations such as image preprocessing to reduce noise, contrast enhancement, and image sharpening. A low-level process is characterized by the fact that both its inputs and outputs are images. Mid-level processing on images involves tasks such as segmentation (partitioning an image into regions or objects), description of those objects to reduce them to a form suitable for computer processing, and classification (recognition) of individual objects. A mid-level process is characterized by the fact that its inputs generally are images, but its outputs are attributes extracted from those images (e.g., edges, contours, and the identity of individual objects). Finally, higher-level processing involves "making sense" of an ensemble of recognized objects, as in image analysis, and, at the far end of the continuum, performing the cognitive functions normally associated with vision.

Based on the preceding comments, we see that a logical place of overlap between image processing and image analysis is the area of recognition of individual regions or objects in an image. Thus, what we call in this book *digital image processing* encompasses processes whose inputs and outputs are images

and, in addition, encompasses processes that extract attributes from images, up to and including the recognition of individual objects. As an illustration to clarify these concepts, consider the area of automated analysis of text. The processes of acquiring an image of the area containing the text, preprocessing that image, extracting (segmenting) the individual characters, describing the characters in a form suitable for computer processing, and recognizing those individual characters are in the scope of what we call digital image processing in this book. Making sense of the content of the page may be viewed as being in the domain of image analysis and even computer vision, depending on the level of complexity implied by the statement "making sense." As will become evident shortly, digital image processing, as we have defined it, is used successfully in a broad range of areas of exceptional social and economic value. The concepts developed in the following chapters are the foundation for the methods used in those application areas.

1.2 The Origins of Digital Image Processing

One of the first applications of digital images was in the newspaper industry, when pictures were first sent by submarine cable between London and New York. Introduction of the Bartlane cable picture transmission system in the early 1920s reduced the time required to transport a picture across the Atlantic from more than a week to less than three hours. Specialized printing equipment coded pictures for cable transmission and then reconstructed them at the receiving end. Figure 1.1 was transmitted in this way and reproduced on a telegraph printer fitted with typefaces simulating a halftone pattern.

Some of the initial problems in improving the visual quality of these early digital pictures were related to the selection of printing procedures and the distribution of intensity levels. The printing method used to obtain Fig. 1.1 was abandoned toward the end of 1921 in favor of a technique based on photographic reproduction made from tapes perforated at the telegraph receiving terminal. Figure 1.2 shows an image obtained using this method. The improvements over Fig. 1.1 are evident, both in tonal quality and in resolution.

FIGURE 1.1 A digital picture produced in 1921 from a coded tape by a telegraph printer with special type faces. (McFarlane.[†])

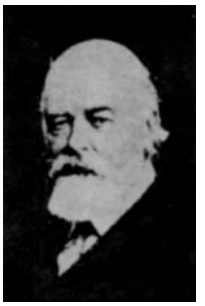

FIGURE 1.2 A digital picture made in 1922 from a tape punched after the signals had crossed the Atlantic twice. (McFarlane.)

The early Bartlane systems were capable of coding images in five distinct levels of gray. This capability was increased to 15 levels in 1929. Figure 1.3 is typical of the type of images that could be obtained using the 15-tone equipment. During this period, introduction of a system for developing a film plate via light beams that were modulated by the coded picture tape improved the reproduction process considerably.

Although the examples just cited involve digital images, they are not considered digital image processing results in the context of our definition because computers were not involved in their creation. Thus, the history of digital image processing is intimately tied to the development of the digital computer. In fact, digital images require so much storage and computational power that progress in the field of digital image processing has been dependent on the development of digital computers and of supporting technologies that include data storage, display, and transmission.

The idea of a computer goes back to the invention of the abacus in Asia Minor, more than 5000 years ago. More recently, there were developments in the past two centuries that are the foundation of what we call a computer today. However, the basis for what we call a *modern* digital computer dates back to only the 1940s with the introduction by John von Neumann of two key concepts: (1) a memory to hold a stored program and data, and (2) conditional branching. These two ideas are the foundation of a central processing unit (CPU), which is at the heart of computers today. Starting with von Neumann, there were a series of key advances that led to computers powerful enough to

FIGURE 1.3 Unretouched cable picture of Generals Pershing and Foch, transmitted in 1929 from London to New York by 15-tone equipment. (McFarlane.)

be used for digital image processing. Briefly, these advances may be summarized as follows: (1) the invention of the transistor at Bell Laboratories in 1948; (2) the development in the 1950s and 1960s of the high-level programming languages COBOL (Common Business-Oriented Language) and FORTRAN (Formula Translator); (3) the invention of the integrated circuit (IC) at Texas Instruments in 1958; (4) the development of operating systems in the early 1960s; (5) the development of the microprocessor (a single chip consisting of the central processing unit, memory, and input and output controls) by Intel in the early 1970s; (6) introduction by IBM of the personal computer in 1981; and (7) progressive miniaturization of components, starting with large scale integration (LI) in the late 1970s, then very large scale integration (VLSI) in the 1980s, to the present use of ultra large scale integration (ULSI). Concurrent with these advances were developments in the areas of mass storage and display systems, both of which are fundamental requirements for digital image processing.

The first computers powerful enough to carry out meaningful image processing tasks appeared in the early 1960s. The birth of what we call digital image processing today can be traced to the availability of those machines and to the onset of the space program during that period. It took the combination of those two developments to bring into focus the potential of digital image processing concepts. Work on using computer techniques for improving images from a space probe began at the Jet Propulsion Laboratory (Pasadena, California) in 1964 when pictures of the moon transmitted by *Ranger 7* were processed by a computer to correct various types of image distortion inherent in the on-board television camera. Figure 1.4 shows the first image of the moon taken by *Ranger 7* on July 31, 1964 at 9:09 A.M. Eastern Daylight Time (EDT), about 17 minutes before impacting the lunar surface (the markers, called *reseau* marks, are used for geometric corrections, as discussed in Chapter 2). This also is the first image of the moon taken by a U.S. spacecraft. The imaging lessons learned with *Ranger 7* served as the basis for improved methods used to enhance and restore images from the Surveyor missions to the moon, the Mariner series of flyby missions to Mars, the Apollo manned flights to the moon, and others.

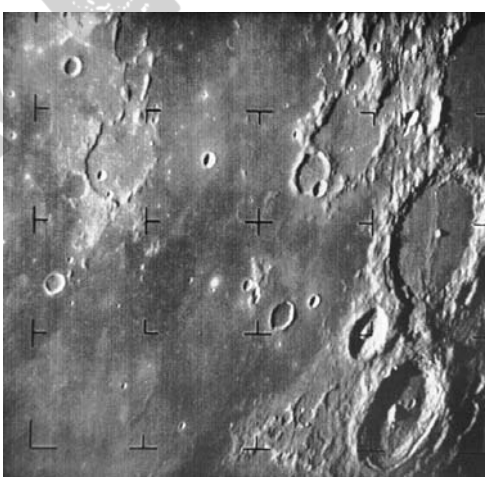

FIGURE 1.4 The first picture of the moon by a U.S. spacecraft. *Ranger 7* took this image on July 31, 1964 at 9:09 A.M. EDT, about 17 minutes before impacting the lunar surface. (Courtesy of NASA.)

In parallel with space applications, digital image processing techniques began in the late 1960s and early 1970s to be used in medical imaging, remote Earth resources observations, and astronomy. The invention in the early 1970s of computerized axial tomography (CAT), also called computerized tomography (CT) for short, is one of the most important events in the application of image processing in medical diagnosis. Computerized axial tomography is a process in which a ring of detectors encircles an object (or patient) and an X-ray source, concentric with the detector ring, rotates about the object. The X-rays pass through the object and are collected at the opposite end by the corresponding detectors in the ring. As the source rotates, this procedure is repeated. Tomography consists of algorithms that use the sensed data to construct an image that represents a "slice" through the object. Motion of the object in a direction perpendicular to the ring of detectors produces a set of such slices, which constitute a three-dimensional (3-D) rendition of the inside of the object. Tomography was invented independently by Sir Godfrey N. Hounsfield and Professor Allan M. Cormack, who shared the 1979 Nobel Prize in Medicine for their invention. It is interesting to note that X-rays were discovered in 1895 by Wilhelm Conrad Roentgen, for which he received the 1901 Nobel Prize for Physics. These two inventions, nearly 100 years apart, led to some of the most important applications of image processing today.

From the 1960s until the present, the field of image processing has grown vigorously. In addition to applications in medicine and the space program, digital image processing techniques now are used in a broad range of applications. Computer procedures are used to enhance the contrast or code the intensity levels into color for easier interpretation of X-rays and other images used in industry, medicine, and the biological sciences. Geographers use the same or similar techniques to study pollution patterns from aerial and satellite imagery. Image enhancement and restoration procedures are used to process degraded images of unrecoverable objects or experimental results too expensive to duplicate. In archeology, image processing methods have successfully restored blurred pictures that were the only available records of rare artifacts lost or damaged after being photographed. In physics and related fields, computer techniques routinely enhance images of experiments in areas such as high-energy plasmas and electron microscopy. Similarly successful applications of image processing concepts can be found in astronomy, biology, nuclear medicine, law enforcement, defense, and industry.

These examples illustrate processing results intended for human interpretation. The second major area of application of digital image processing techniques mentioned at the beginning of this chapter is in solving problems dealing with machine perception. In this case, interest is on procedures for extracting from an image information in a form suitable for computer processing. Often, this information bears little resemblance to visual features that humans use in interpreting the content of an image. Examples of the type of information used in machine perception are statistical moments, Fourier transform coefficients, and multidimensional distance measures. Typical problems in machine perception that routinely utilize image processing techniques are automatic character recognition, industrial machine vision for product assembly and inspection,

military recognizance, automatic processing of fingerprints, screening of X-rays and blood samples, and machine processing of aerial and satellite imagery for weather prediction and environmental assessment. The continuing decline in the ratio of computer price to performance and the expansion of networking and communication bandwidth via the World Wide Web and the Internet have created unprecedented opportunities for continued growth of digital image processing. Some of these application areas are illustrated in the following section.

1.3 Examples of Fields that Use Digital Image Processing

Today, there is almost no area of technical endeavor that is not impacted in some way by digital image processing. We can cover only a few of these applications in the context and space of the current discussion. However, limited as it is, the material presented in this section will leave no doubt in your mind regarding the breadth and importance of digital image processing. We show in this section numerous areas of application, each of which routinely utilizes the digital image processing techniques developed in the following chapters. Many of the images shown in this section are used later in one or more of the examples given in the book. All images shown are digital.

The areas of application of digital image processing are so varied that some form of organization is desirable in attempting to capture the breadth of this field. One of the simplest ways to develop a basic understanding of the extent of image processing applications is to categorize images according to their source (e.g., visual, X-ray, and so on). The principal energy source for images in use today is the electromagnetic energy spectrum. Other important sources of energy include acoustic, ultrasonic, and electronic (in the form of electron beams used in electron microscopy). Synthetic images, used for modeling and visualization, are generated by computer. In this section we discuss briefly how images are generated in these various categories and the areas in which they are applied. Methods for converting images into digital form are discussed in the next chapter.

Images based on radiation from the EM spectrum are the most familiar, especially images in the X-ray and visual bands of the spectrum. Electromagnetic waves can be conceptualized as propagating sinusoidal waves of varying wavelengths, or they can be thought of as a stream of massless particles, each traveling in a wavelike pattern and moving at the speed of light. Each massless particle contains a certain amount (or bundle) of energy. Each bundle of energy is called a *photon*. If spectral bands are grouped according to energy per photon, we obtain the spectrum shown in Fig. 1.5, ranging from gamma rays (highest energy) at one end to radio waves (lowest energy) at the other.

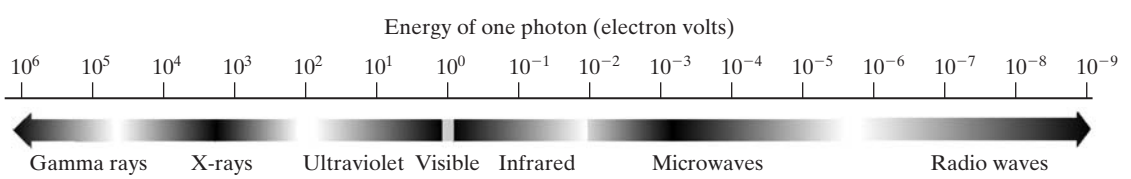

FIGURE 1.5 The electromagnetic spectrum arranged according to energy per photon.

The bands are shown shaded to convey the fact that bands of the EM spectrum are not distinct but rather transition smoothly from one to the other.

1.3.1 Gamma-Ray Imaging

Major uses of imaging based on gamma rays include nuclear medicine and astronomical observations. In nuclear medicine, the approach is to inject a patient with a radioactive isotope that emits gamma rays as it decays. Images are produced from the emissions collected by gamma ray detectors. Figure 1.6(a) shows an image of a complete bone scan obtained by using gamma-ray imaging. Images of this sort are used to locate sites of bone pathology, such as infections

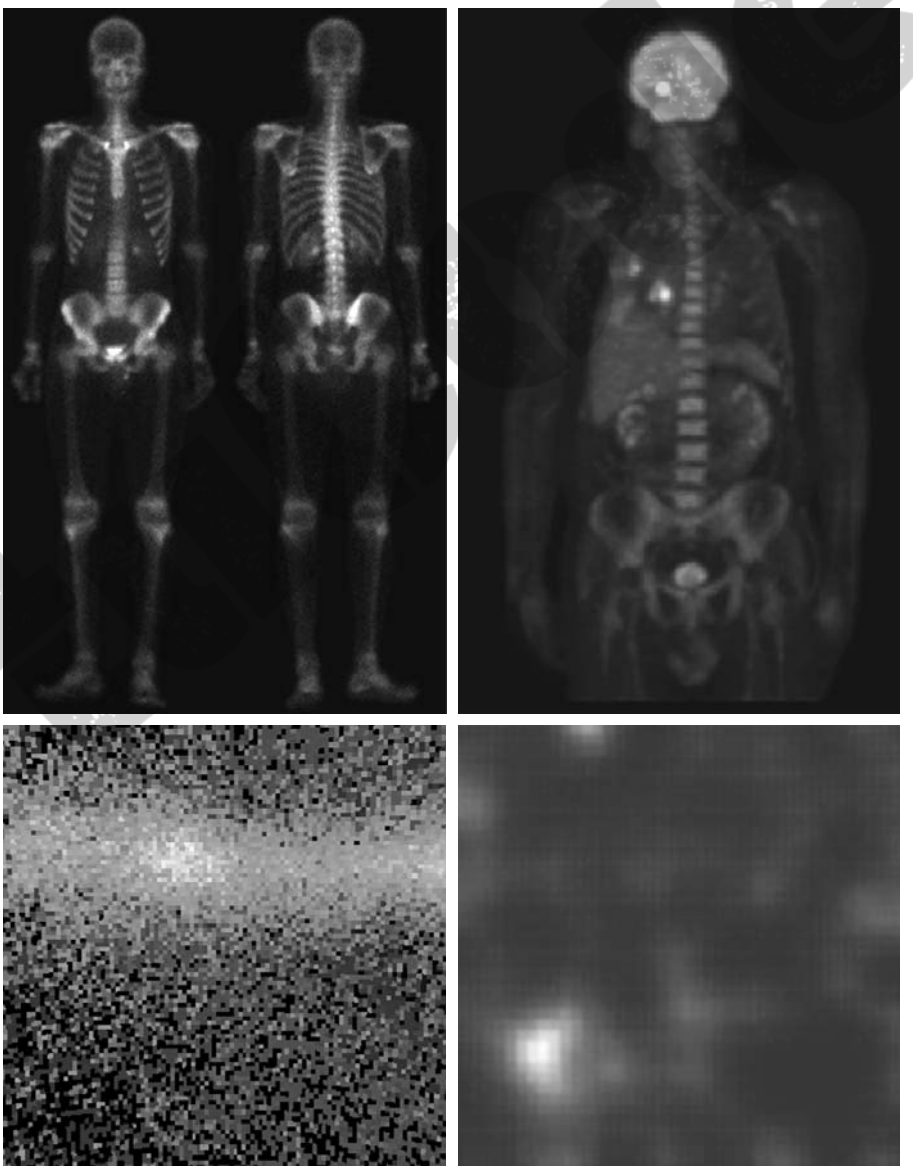

a b
c d

FIGURE 1.6
Examples of gamma-ray imaging. (a) Bone scan. (b) PET image. (c) Cygnus Loop. (d) Gamma radiation (bright spot) from a reactor valve. (Images courtesy of (a) G.E. Medical Systems, (b) Dr. Michael E. Casey, CTI PET Systems, (c) NASA, (d) Professors Zhong He and David K. Wehe, University of Michigan.)

or tumors. Figure 1.6(b) shows another major modality of nuclear imaging called positron emission tomography (PET). The principle is the same as with X-ray tomography, mentioned briefly in Section 1.2. However, instead of using an external source of X-ray energy, the patient is given a radioactive isotope that emits positrons as it decays. When a positron meets an electron, both are annihilated and two gamma rays are given off. These are detected and a tomographic image is created using the basic principles of tomography. The image shown in Fig. 1.6(b) is one sample of a sequence that constitutes a 3-D rendition of the patient. This image shows a tumor in the brain and one in the lung, easily visible as small white masses.

A star in the constellation of Cygnus exploded about 15,000 years ago, generating a superheated stationary gas cloud (known as the Cygnus Loop) that glows in a spectacular array of colors. Figure 1.6(c) shows an image of the Cygnus Loop in the gamma-ray band. Unlike the two examples in Figs. 1.6(a) and (b), this image was obtained using the natural radiation of the object being imaged. Finally, Fig. 1.6(d) shows an image of gamma radiation from a valve in a nuclear reactor. An area of strong radiation is seen in the lower left side of the image.

1.3.2 X-Ray Imaging

X-rays are among the oldest sources of EM radiation used for imaging. The best known use of X-rays is medical diagnostics, but they also are used extensively in industry and other areas, like astronomy. X-rays for medical and industrial imaging are generated using an X-ray tube, which is a vacuum tube with a cathode and anode. The cathode is heated, causing free electrons to be released. These electrons flow at high speed to the positively charged anode. When the electrons strike a nucleus, energy is released in the form of X-ray radiation. The energy (penetrating power) of X-rays is controlled by a voltage applied across the anode, and by a current applied to the filament in the cathode. Figure 1.7(a) shows a familiar chest X-ray generated simply by placing the patient between an X-ray source and a film sensitive to X-ray energy. The intensity of the X-rays is modified by absorption as they pass through the patient, and the resulting energy falling on the film develops it, much in the same way that light develops photographic film. In digital radiography, digital images are obtained by one of two methods: (1) by digitizing X-ray films; or (2) by having the X-rays that pass through the patient fall directly onto devices (such as a phosphor screen) that convert X-rays to light. The light signal in turn is captured by a light-sensitive digitizing system. We discuss digitization in more detail in Chapters 2 and 4.

Angiography is another major application in an area called contrast-enhancement radiography. This procedure is used to obtain images (called *angiograms*) of blood vessels. A catheter (a small, flexible, hollow tube) is inserted, for example, into an artery or vein in the groin. The catheter is threaded into the blood vessel and guided to the area to be studied. When the catheter reaches the site under investigation, an X-ray contrast medium is injected through the tube. This enhances contrast of the blood vessels and enables the radiologist to see any irregularities or blockages. Figure 1.7(b) shows an example of an aortic angiogram. The catheter can be seen being inserted into the

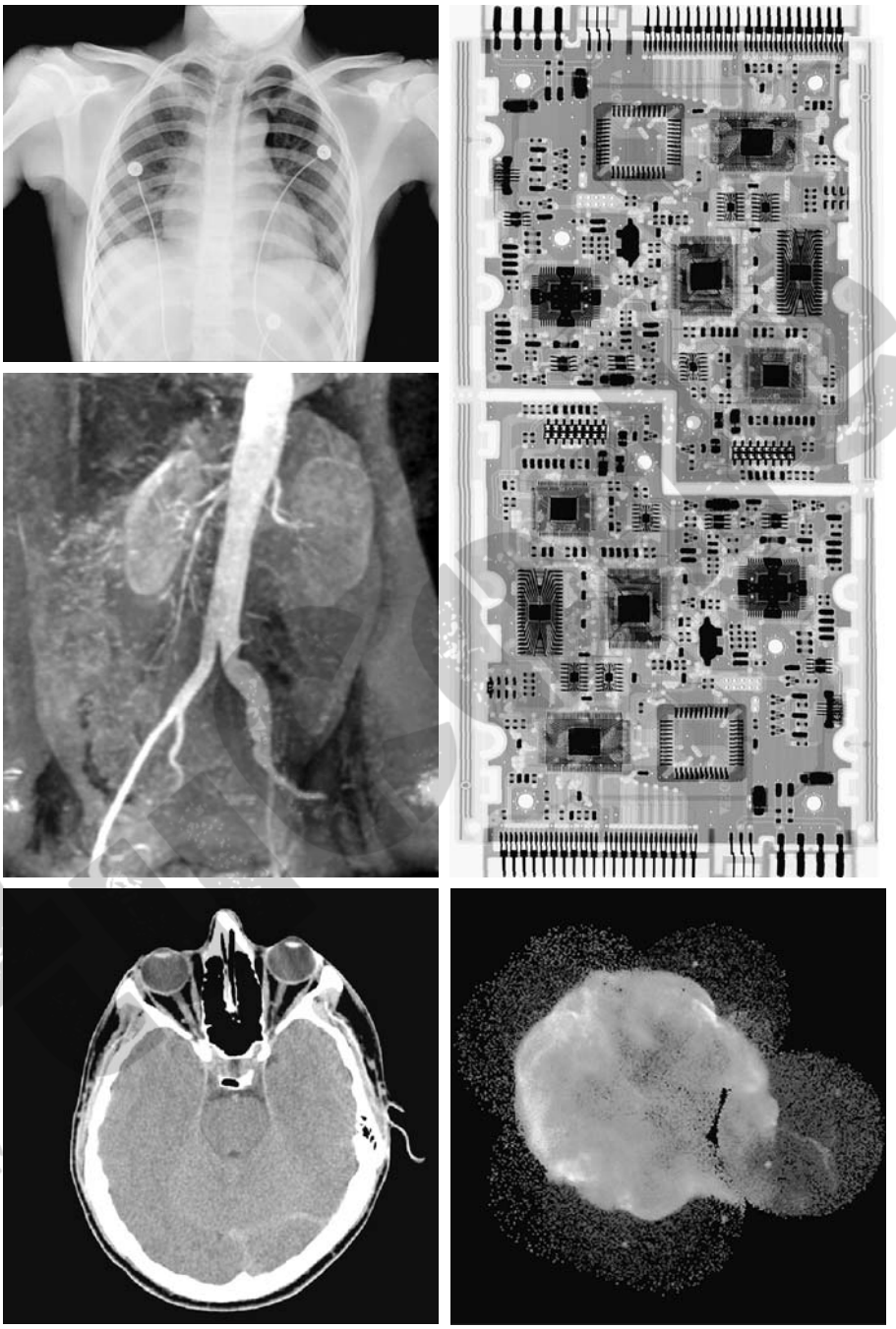

a d
b
c e

FIGURE 1.7 Examples of X-ray imaging. (a) Chest X-ray. (b) Aortic angiogram. (c) Head CT. (d) Circuit boards. (e) Cygnus Loop. (Images courtesy of (a) and (c) Dr. David R. Pickens, Dept. of Radiology & Radiological Sciences, Vanderbilt University Medical Center; (b) Dr. Thomas R. Gest, Division of Anatomical Sciences, University of Michigan Medical School; (d) Mr. Joseph E. Pascente, Lixi, Inc.; and (e) NASA.)

large blood vessel on the lower left of the picture. Note the high contrast of the large vessel as the contrast medium flows up in the direction of the kidneys, which are also visible in the image. As discussed in Chapter 2, angiography is a major area of digital image processing, where image subtraction is used to enhance further the blood vessels being studied.

Another important use of X-rays in medical imaging is computerized axial tomography (CAT). Due to their resolution and 3-D capabilities, CAT scans revolutionized medicine from the moment they first became available in the early 1970s. As noted in Section 1.2, each CAT image is a "slice" taken perpendicularly through the patient. Numerous slices are generated as the patient is moved in a longitudinal direction. The ensemble of such images constitutes a 3-D rendition of the inside of the body, with the longitudinal resolution being proportional to the number of slice images taken. Figure 1.7(c) shows a typical head CAT slice image.

Techniques similar to the ones just discussed, but generally involving higher-energy X-rays, are applicable in industrial processes. Figure 1.7(d) shows an X-ray image of an electronic circuit board. Such images, representative of literally hundreds of industrial applications of X-rays, are used to examine circuit boards for flaws in manufacturing, such as missing components or broken traces. Industrial CAT scans are useful when the parts can be penetrated by X-rays, such as in plastic assemblies, and even large bodies, like solid-propellant rocket motors. Figure 1.7(e) shows an example of X-ray imaging in astronomy. This image is the Cygnus Loop of Fig. 1.6(c), but imaged this time in the X-ray band.

1.3.3 Imaging in the Ultraviolet Band

Applications of ultraviolet "light" are varied. They include lithography, industrial inspection, microscopy, lasers, biological imaging, and astronomical observations. We illustrate imaging in this band with examples from microscopy and astronomy.

Ultraviolet light is used in fluorescence microscopy, one of the fastest growing areas of microscopy. Fluorescence is a phenomenon discovered in the middle of the nineteenth century, when it was first observed that the mineral fluorspar fluoresces when ultraviolet light is directed upon it. The ultraviolet light itself is not visible, but when a photon of ultraviolet radiation collides with an electron in an atom of a fluorescent material, it elevates the electron to a higher energy level. Subsequently, the excited electron relaxes to a lower level and emits light in the form of a lower-energy photon in the visible (red) light region. The basic task of the fluorescence microscope is to use an excitation light to irradiate a prepared specimen and then to separate the much weaker radiating fluorescent light from the brighter excitation light. Thus, only the emission light reaches the eye or other detector. The resulting fluorescing areas shine against a dark background with sufficient contrast to permit detection. The darker the background of the nonfluorescing material, the more efficient the instrument.

Fluorescence microscopy is an excellent method for studying materials that can be made to fluoresce, either in their natural form (primary fluorescence) or when treated with chemicals capable of fluorescing (secondary fluorescence). Figures 1.8(a) and (b) show results typical of the capability of fluorescence microscopy. Figure 1.8(a) shows a fluorescence microscope image of normal corn, and Fig. 1.8(b) shows corn infected by "smut," a disease of cereals, corn,

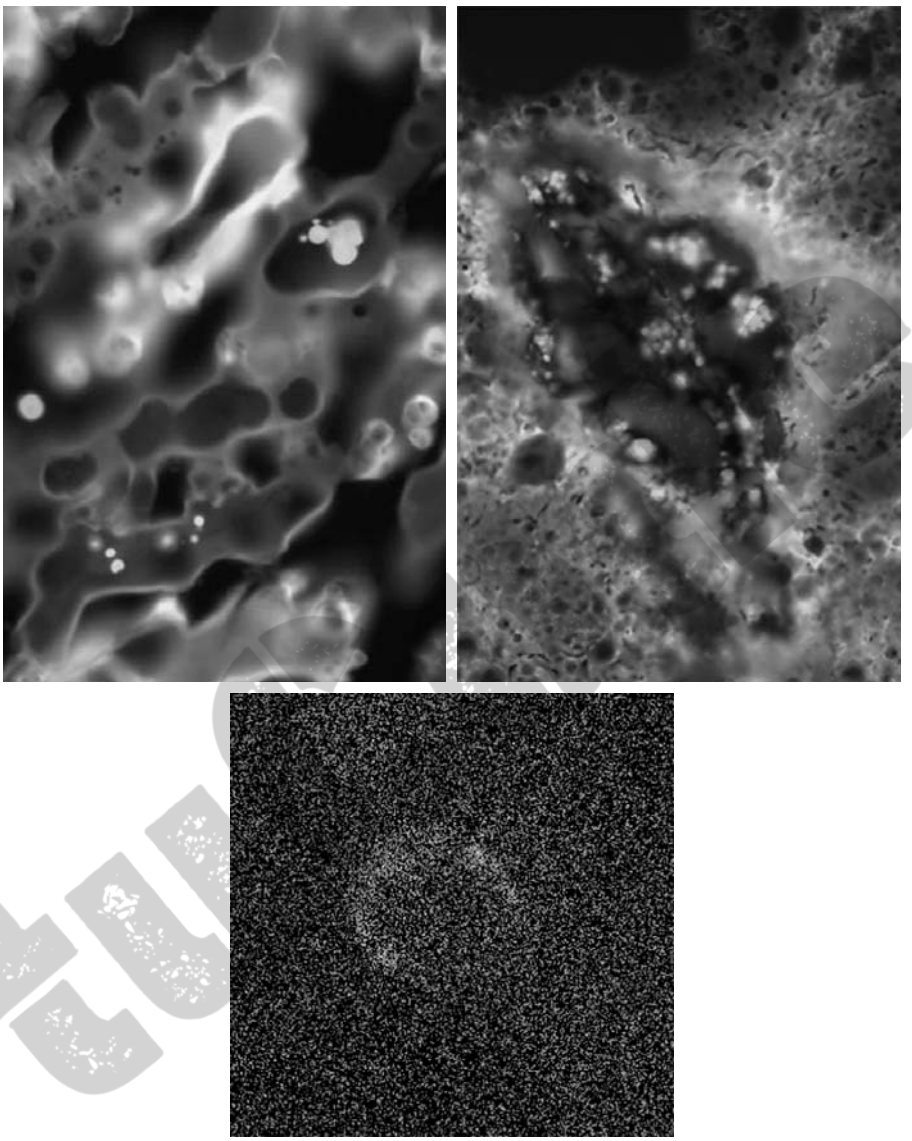

a b
c

FIGURE 1.8
Examples of ultraviolet imaging.
(a) Normal corn.
(b) Smut corn.
(c) Cygnus Loop.
(Images courtesy of (a) and (b) Dr. Michael W. Davidson, Florida State University, (c) NASA.)

grasses, onions, and sorghum that can be caused by any of more than 700 species of parasitic fungi. Corn smut is particularly harmful because corn is one of the principal food sources in the world. As another illustration, Fig. 1.8(c) shows the Cygnus Loop imaged in the high-energy region of the ultraviolet band.

1.3.4 Imaging in the Visible and Infrared Bands

Considering that the visual band of the electromagnetic spectrum is the most familiar in all our activities, it is not surprising that imaging in this band outweighs by far all the others in terms of breadth of application. The infrared band often is used in conjunction with visual imaging, so we have grouped the

visible and infrared bands in this section for the purpose of illustration. We consider in the following discussion applications in light microscopy, astronomy, remote sensing, industry, and law enforcement.

Figure 1.9 shows several examples of images obtained with a light microscope. The examples range from pharmaceuticals and microinspection to materials characterization. Even in microscopy alone, the application areas are too numerous to detail here. It is not difficult to conceptualize the types of processes one might apply to these images, ranging from enhancement to measurements.

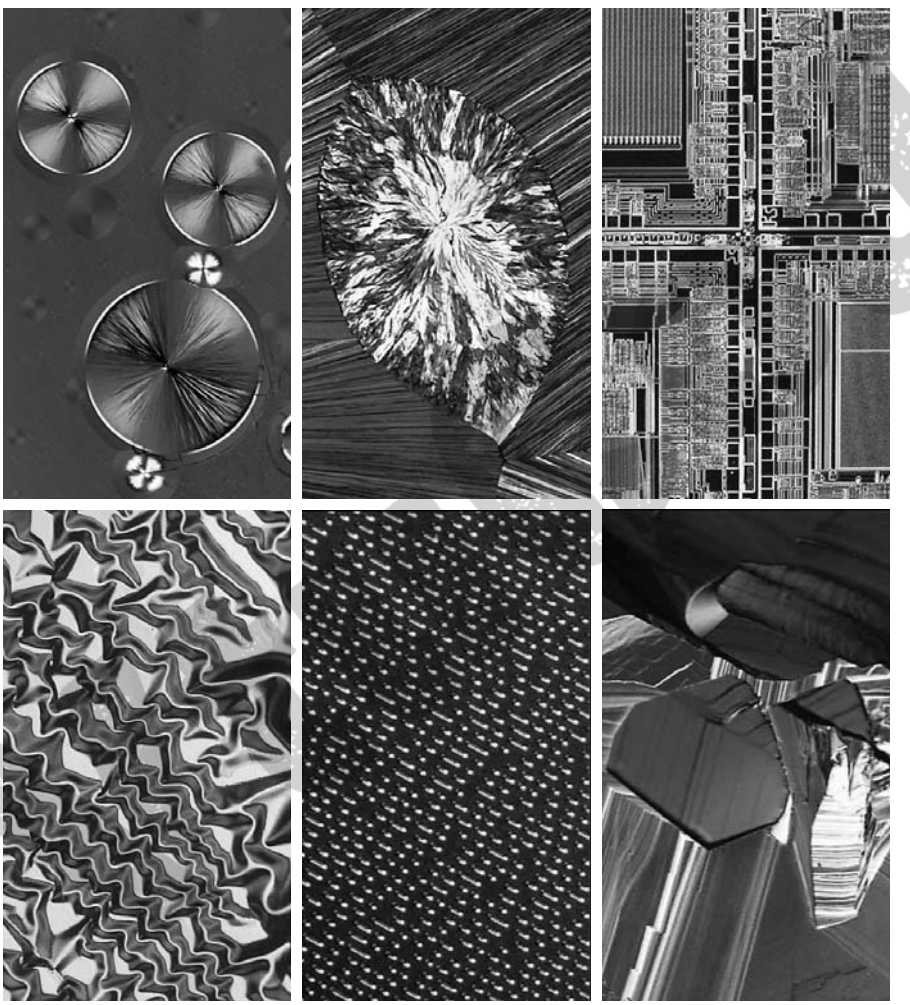

a b c
d e f

FIGURE 1.9 Examples of light microscopy images. (a) Taxol (anticancer agent), magnified 250×. (b) Cholesterol—40×. (c) Microprocessor—60×. (d) Nickel oxide thin film—600×. (e) Surface of audio CD—1750×. (f) Organic superconductor—450×. (Images courtesy of Dr. Michael W. Davidson, Florida State University.)

TABLE 1.1 Thematic bands in NASA's LANDSAT satellite.

Band No.	Name	Wavelength (μm)	Characteristics and Uses
1	Visible blue	0.45–0.52	Maximum water penetration
2	Visible green	0.52–0.60	Good for measuring plant vigor
3	Visible red	0.63–0.69	Vegetation discrimination
4	Near infrared	0.76–0.90	Biomass and shoreline mapping
5	Middle infrared	1.55–1.75	Moisture content of soil and vegetation
6	Thermal infrared	10.4–12.5	Soil moisture; thermal mapping
7	Middle infrared	2.08–2.35	Mineral mapping

Another major area of visual processing is remote sensing, which usually includes several bands in the visual and infrared regions of the spectrum. Table 1.1 shows the so-called *thematic bands* in NASA's LANDSAT satellite. The primary function of LANDSAT is to obtain and transmit images of the Earth from space for purposes of monitoring environmental conditions on the planet. The bands are expressed in terms of wavelength, with 1 μm being equal to 10^{-6} m (we discuss the wavelength regions of the electromagnetic spectrum in more detail in Chapter 2). Note the characteristics and uses of each band in Table 1.1.

In order to develop a basic appreciation for the power of this type of *multispectral* imaging, consider Fig. 1.10, which shows one image for each of

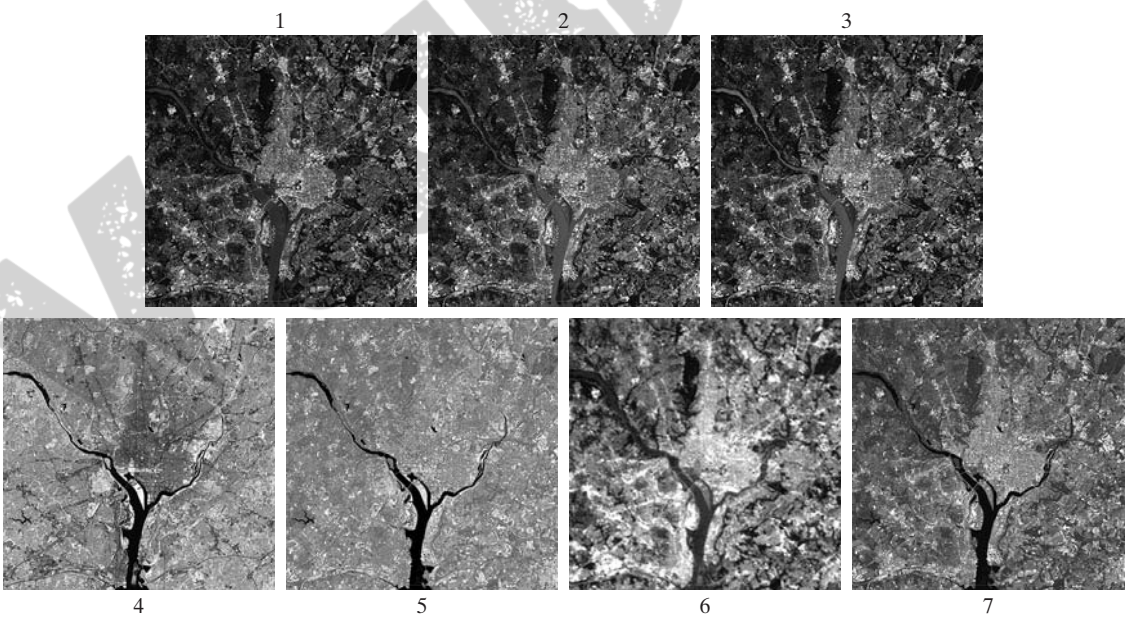

FIGURE 1.10 LANDSAT satellite images of the Washington, D.C. area. The numbers refer to the thematic bands in Table 1.1. (Images courtesy of NASA.)

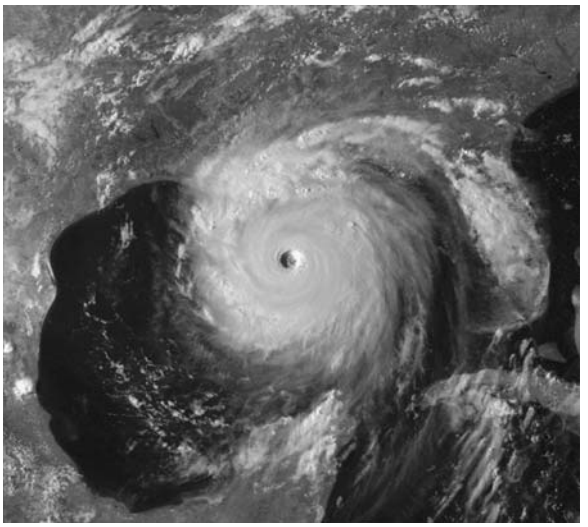

FIGURE 1.11 Satellite image of Hurricane Katrina taken on August 29, 2005. (Courtesy of NOAA.)

the spectral bands in Table 1.1. The area imaged is Washington D.C., which includes features such as buildings, roads, vegetation, and a major river (the Potomac) going though the city. Images of population centers are used routinely (over time) to assess population growth and shift patterns, pollution, and other factors harmful to the environment. The differences between visual and infrared image features are quite noticeable in these images. Observe, for example, how well defined the river is from its surroundings in Bands 4 and 5.

Weather observation and prediction also are major applications of multispectral imaging from satellites. For example, Fig. 1.11 is an image of Hurricane Katrina one of the most devastating storms in recent memory in the Western Hemisphere. This image was taken by a National Oceanographic and Atmospheric Administration (NOAA) satellite using sensors in the visible and infrared bands. The eye of the hurricane is clearly visible in this image.

Figures 1.12 and 1.13 show an application of infrared imaging. These images are part of the *Nighttime Lights of the World* data set, which provides a global inventory of human settlements. The images were generated by the infrared imaging system mounted on a NOAA DMSP (Defense Meteorological Satellite Program) satellite. The infrared imaging system operates in the band 10.0 to 13.4 μm, and has the unique capability to observe faint sources of visible-near infrared emissions present on the Earth's surface, including cities, towns, villages, gas flares, and fires. Even without formal training in image processing, it is not difficult to imagine writing a computer program that would use these images to estimate the percent of total electrical energy used by various regions of the world.

A major area of imaging in the visual spectrum is in automated visual inspection of manufactured goods. Figure 1.14 shows some examples. Figure 1.14(a) is a controller board for a CD-ROM drive. A typical image processing task with products like this is to inspect them for missing parts (the black square on the top, right quadrant of the image is an example of a missing component).

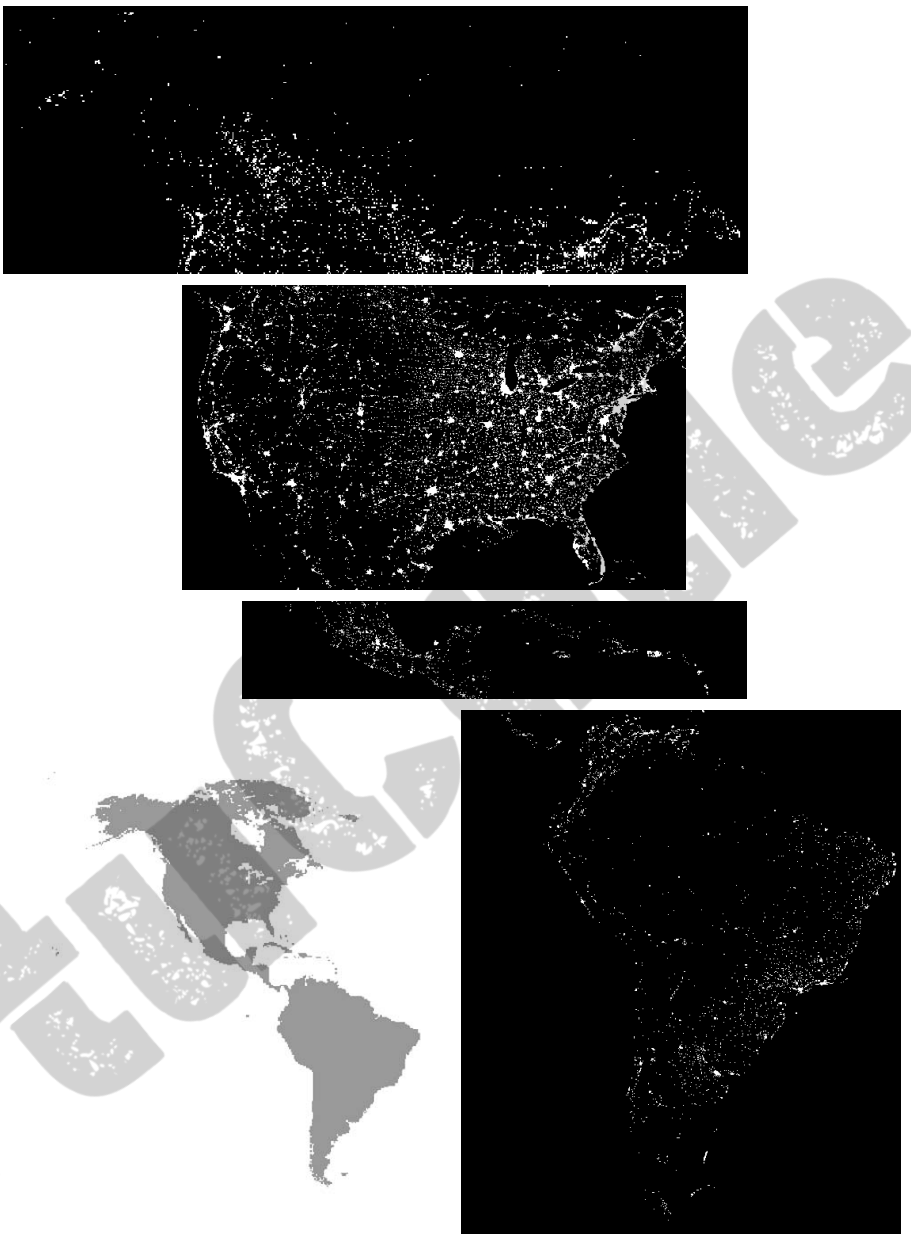

FIGURE 1.12
Infrared satellite images of the Americas. The small gray map is provided for reference. (Courtesy of NOAA.)

Figure 1.14(b) is an imaged pill container. The objective here is to have a machine look for missing pills. Figure 1.14(c) shows an application in which image processing is used to look for bottles that are not filled up to an acceptable level. Figure 1.14(d) shows a clear-plastic part with an unacceptable number of air pockets in it. Detecting anomalies like these is a major theme of industrial inspection that includes other products such as wood and cloth. Figure 1.14(e)

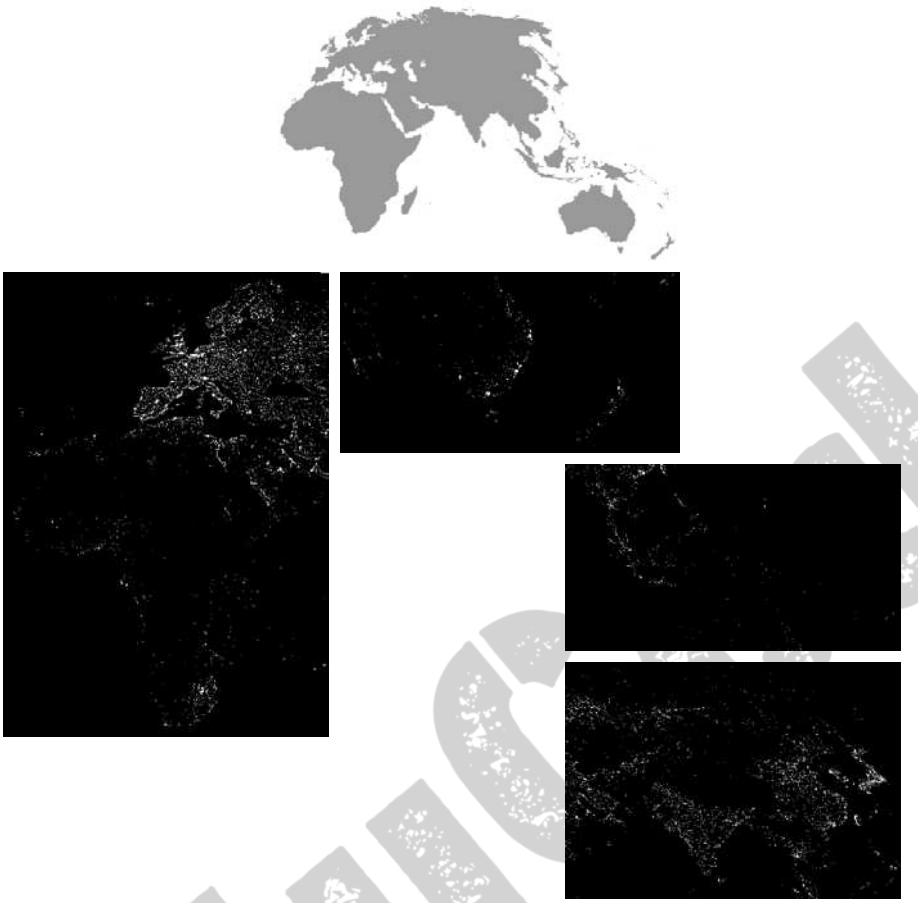

FIGURE 1.13 Infrared satellite images of the remaining populated part of the world. The small gray map is provided for reference. (Courtesy of NOAA.)

shows a batch of cereal during inspection for color and the presence of anomalies such as burned flakes. Finally, Fig. 1.14(f) shows an image of an intraocular implant (replacement lens for the human eye). A "structured light" illumination technique was used to highlight for easier detection flat lens deformations toward the center of the lens. The markings at 1 o'clock and 5 o'clock are tweezer damage. Most of the other small speckle detail is debris. The objective in this type of inspection is to find damaged or incorrectly manufactured implants automatically, prior to packaging.

As a final illustration of image processing in the visual spectrum, consider Fig. 1.15. Figure 1.15(a) shows a thumb print. Images of fingerprints are routinely processed by computer, either to enhance them or to find features that aid in the automated search of a database for potential matches. Figure 1.15(b) shows an image of paper currency. Applications of digital image processing in this area include automated counting and, in law enforcement, the reading of the serial number for the purpose of tracking and identifying bills. The two vehicle images shown in Figs. 1.15 (c) and (d) are examples of automated license plate reading. The light rectangles indicate the area in which the imaging system

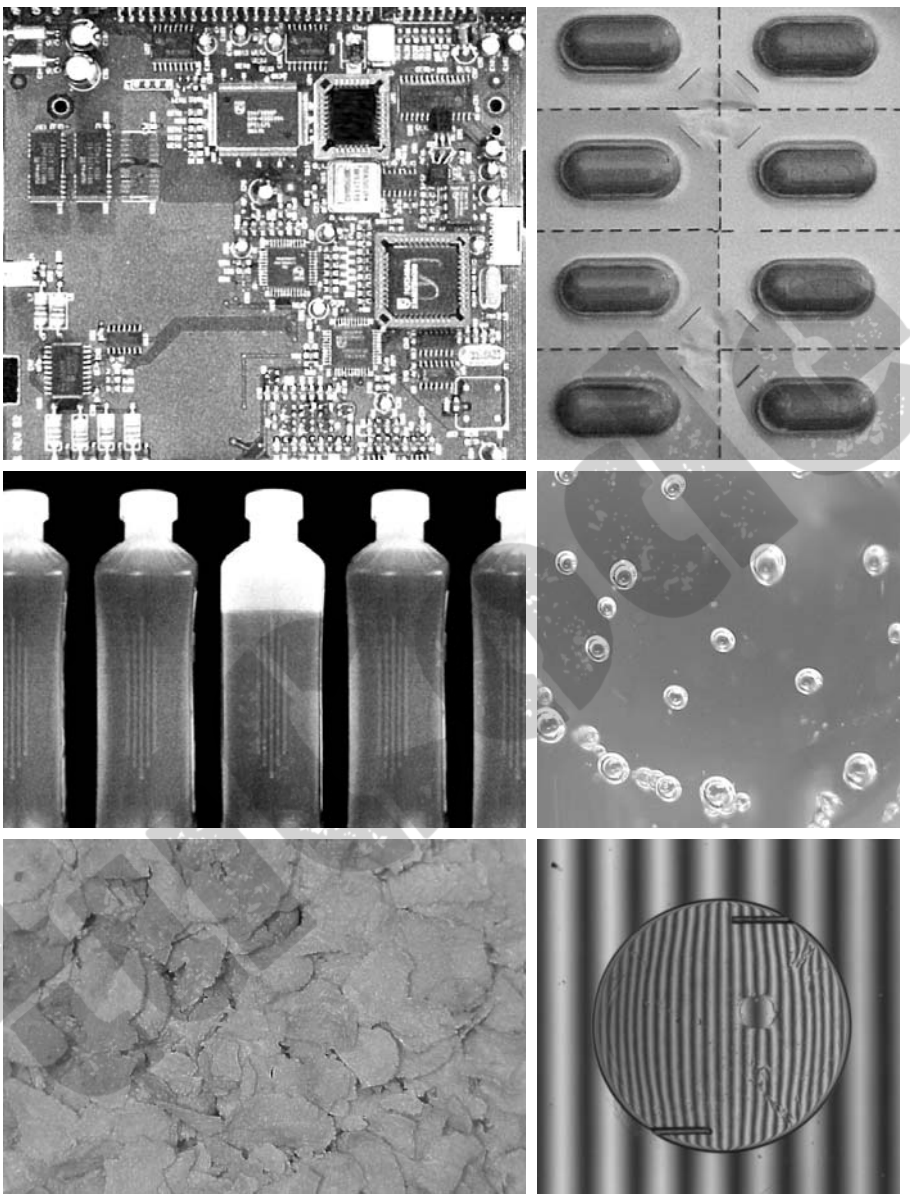

a b
c d
e f

FIGURE 1.14
Some examples of manufactured goods often checked using digital image processing. (a) A circuit board controller. (b) Packaged pills. (c) Bottles. (d) Air bubbles in a clear-plastic product. (e) Cereal. (f) Image of intraocular implant. (Fig. (f) courtesy of Mr. Pete Sites, Perceptics Corporation.)

detected the plate. The black rectangles show the results of automated reading of the plate content by the system. License plate and other applications of character recognition are used extensively for traffic monitoring and surveillance.

1.3.5 Imaging in the Microwave Band

The dominant application of imaging in the microwave band is radar. The unique feature of imaging radar is its ability to collect data over virtually any region at any time, regardless of weather or ambient lighting conditions. Some

a b
c
d

FIGURE 1.15
Some additional examples of imaging in the visual spectrum. (a) Thumb print. (b) Paper currency. (c) and (d) Automated license plate reading. (Figure (a) courtesy of the National Institute of Standards and Technology. Figures (c) and (d) courtesy of Dr. Juan Herrera, Perceptics Corporation.)

radar waves can penetrate clouds, and under certain conditions can also see through vegetation, ice, and dry sand. In many cases, radar is the only way to explore inaccessible regions of the Earth's surface. An imaging radar works like a flash camera in that it provides its own illumination (microwave pulses) to illuminate an area on the ground and take a snapshot image. Instead of a camera lens, a radar uses an antenna and digital computer processing to record its images. In a radar image, one can see only the microwave energy that was reflected back toward the radar antenna.

Figure 1.16 shows a spaceborne radar image covering a rugged mountainous area of southeast Tibet, about 90 km east of the city of Lhasa. In the lower right corner is a wide valley of the Lhasa River, which is populated by Tibetan farmers and yak herders and includes the village of Menba. Mountains in this area reach about 5800 m (19,000 ft) above sea level, while the valley floors lie about 4300 m (14,000 ft) above sea level. Note the clarity and detail of the image, unencumbered by clouds or other atmospheric conditions that normally interfere with images in the visual band.

FIGURE 1.16
Spaceborne radar image of mountains in southeast Tibet. (Courtesy of NASA.)

1.3.6 Imaging in the Radio Band

As in the case of imaging at the other end of the spectrum (gamma rays), the major applications of imaging in the radio band are in medicine and astronomy. In medicine, radio waves are used in magnetic resonance imaging (MRI). This technique places a patient in a powerful magnet and passes radio waves through his or her body in short pulses. Each pulse causes a responding pulse of radio waves to be emitted by the patient's tissues. The location from which these signals originate and their strength are determined by a computer, which produces a two-dimensional picture of a section of the patient. MRI can produce pictures in any plane. Figure 1.17 shows MRI images of a human knee and spine.

The last image to the right in Fig. 1.18 shows an image of the Crab Pulsar in the radio band. Also shown for an interesting comparison are images of the same region but taken in most of the bands discussed earlier. Note that each image gives a totally different "view" of the Pulsar.

1.3.7 Examples in which Other Imaging Modalities Are Used

Although imaging in the electromagnetic spectrum is dominant by far, there are a number of other imaging modalities that also are important. Specifically, we discuss in this section acoustic imaging, electron microscopy, and synthetic (computer-generated) imaging.

Imaging using "sound" finds application in geological exploration, industry, and medicine. Geological applications use sound in the low end of the sound spectrum (hundreds of Hz) while imaging in other areas use ultrasound (millions of Hz). The most important commercial applications of image processing in geology are in mineral and oil exploration. For image acquisition over land, one of the main approaches is to use a large truck and a large flat steel plate. The plate is pressed on the ground by the truck, and the truck is vibrated through a frequency spectrum up to 100 Hz. The strength and speed of the

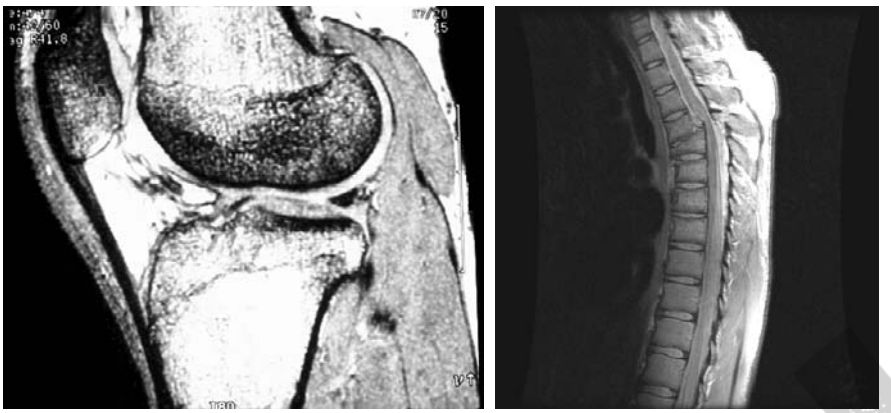

a b

FIGURE 1.17 MRI images of a human (a) knee, and (b) spine. (Image (a) courtesy of Dr. Thomas R. Gest, Division of Anatomical Sciences, University of Michigan Medical School, and (b) courtesy of Dr. David R. Pickens, Department of Radiology and Radiological Sciences, Vanderbilt University Medical Center.)

returning sound waves are determined by the composition of the Earth below the surface. These are analyzed by computer, and images are generated from the resulting analysis.

For marine acquisition, the energy source consists usually of two air guns towed behind a ship. Returning sound waves are detected by hydrophones placed in cables that are either towed behind the ship, laid on the bottom of the ocean, or hung from buoys (vertical cables). The two air guns are alternately pressurized to ~2000 psi and then set off. The constant motion of the ship provides a transversal direction of motion that, together with the returning sound waves, is used to generate a 3-D map of the composition of the Earth below the bottom of the ocean.

Figure 1.19 shows a cross-sectional image of a well-known 3-D model against which the performance of seismic imaging algorithms is tested. The arrow points to a hydrocarbon (oil and/or gas) trap. This target is brighter than the surrounding layers because the change in density in the target region is

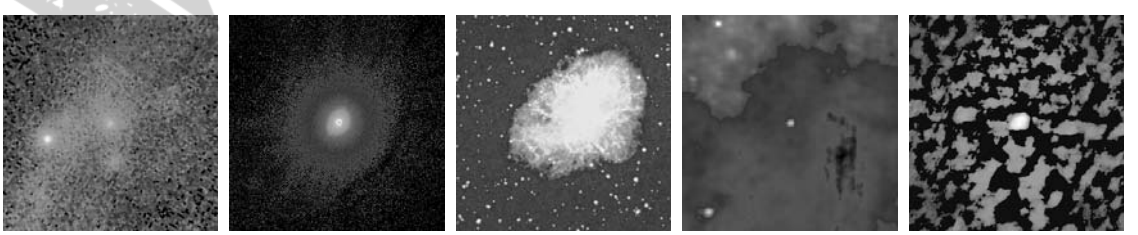

Gamma X-ray Optical Infrared Radio

FIGURE 1.18 Images of the Crab Pulsar (in the center of each image) covering the electromagnetic spectrum. (Courtesy of NASA.)

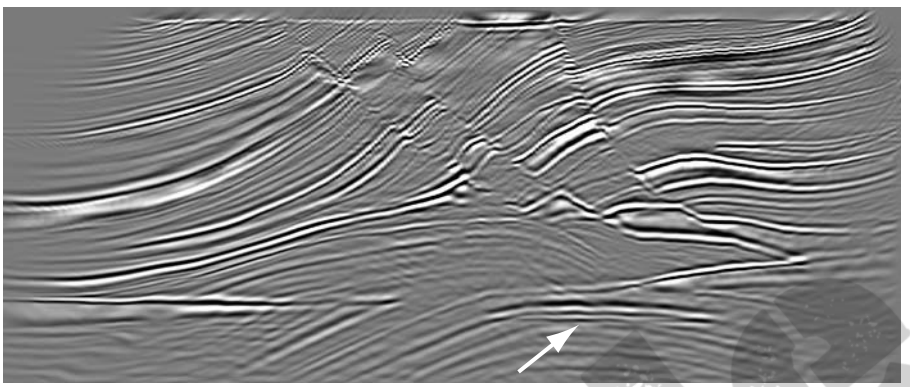

FIGURE 1.19
Cross-sectional image of a seismic model. The arrow points to a hydrocarbon (oil and/or gas) trap. (Courtesy of Dr. Curtis Ober, Sandia National Laboratories.)

larger. Seismic interpreters look for these "bright spots" to find oil and gas. The layers above also are bright, but their brightness does not vary as strongly across the layers. Many seismic reconstruction algorithms have difficulty imaging this target because of the faults above it.

Although ultrasound imaging is used routinely in manufacturing, the best known applications of this technique are in medicine, especially in obstetrics, where unborn babies are imaged to determine the health of their development. A byproduct of this examination is determining the sex of the baby. Ultrasound images are generated using the following basic procedure:

1. The ultrasound system (a computer, ultrasound probe consisting of a source and receiver, and a display) transmits high-frequency (1 to 5 MHz) sound pulses into the body.
2. The sound waves travel into the body and hit a boundary between tissues (e.g., between fluid and soft tissue, soft tissue and bone). Some of the sound waves are reflected back to the probe, while some travel on further until they reach another boundary and get reflected.
3. The reflected waves are picked up by the probe and relayed to the computer.
4. The machine calculates the distance from the probe to the tissue or organ boundaries using the speed of sound in tissue (1540 m/s) and the time of each echo's return.
5. The system displays the distances and intensities of the echoes on the screen, forming a two-dimensional image.

In a typical ultrasound image, millions of pulses and echoes are sent and received each second. The probe can be moved along the surface of the body and angled to obtain various views. Figure 1.20 shows several examples.

We continue the discussion on imaging modalities with some examples of electron microscopy. Electron microscopes function as their optical counterparts, except that they use a focused beam of electrons instead of light to image a specimen. The operation of electron microscopes involves the following basic steps: A stream of electrons is produced by an electron source and accelerated toward the specimen using a positive electrical potential. This stream

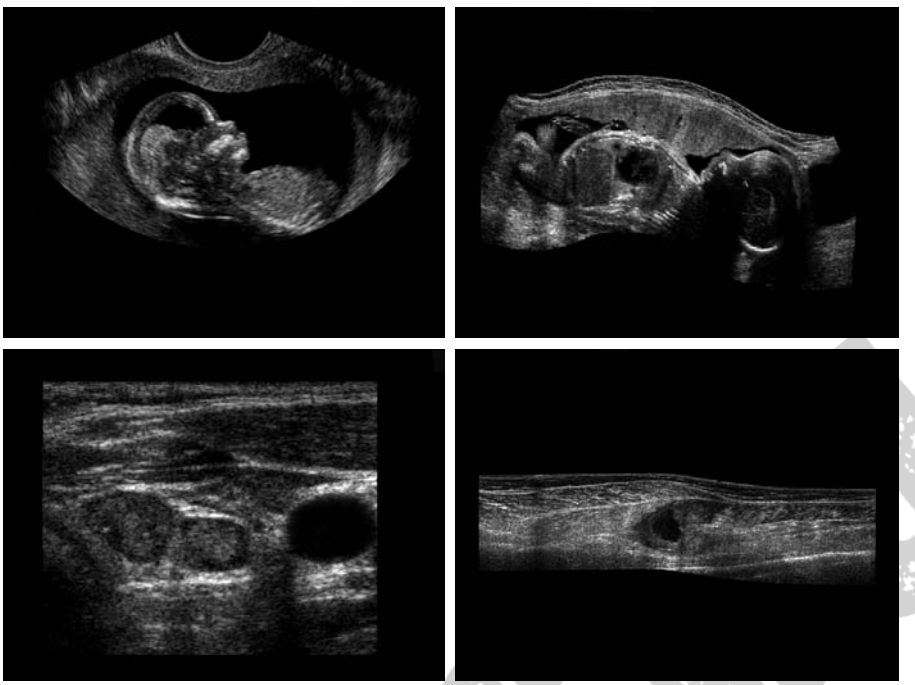

a b
c d

FIGURE 1.20 Examples of ultrasound imaging. (a) Baby. (b) Another view of baby. (c) Thyroids. (d) Muscle layers showing lesion. (Courtesy of Siemens Medical Systems, Inc., Ultrasound Group.)

is confined and focused using metal apertures and magnetic lenses into a thin, monochromatic beam. This beam is focused onto the sample using a magnetic lens. Interactions occur inside the irradiated sample, affecting the electron beam. These interactions and effects are detected and transformed into an image, much in the same way that light is reflected from, or absorbed by, objects in a scene. These basic steps are carried out in all electron microscopes.

A *transmission electron microscope* (TEM) works much like a slide projector. A projector shines (transmits) a beam of light through a slide; as the light passes through the slide, it is modulated by the contents of the slide. This transmitted beam is then projected onto the viewing screen, forming an enlarged image of the slide. TEMs work the same way, except that they shine a beam of electrons through a specimen (analogous to the slide). The fraction of the beam transmitted through the specimen is projected onto a phosphor screen. The interaction of the electrons with the phosphor produces light and, therefore, a viewable image. A *scanning electron microscope* (SEM), on the other hand, actually scans the electron beam and records the interaction of beam and sample at each location. This produces one dot on a phosphor screen. A complete image is formed by a raster scan of the beam through the sample, much like a TV camera. The electrons interact with a phosphor screen and produce light. SEMs are suitable for "bulky" samples, while TEMs require very thin samples.

Electron microscopes are capable of very high magnification. While light microscopy is limited to magnifications on the order 1000×, electron microscopes

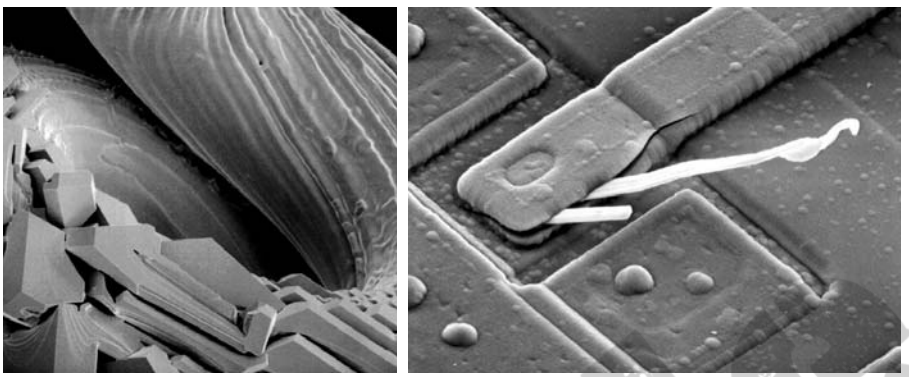

a b

FIGURE 1.21 (a) 250× SEM image of a tungsten filament following thermal failure (note the shattered pieces on the lower left). (b) 2500× SEM image of damaged integrated circuit. The white fibers are oxides resulting from thermal destruction. (Figure (a) courtesy of Mr. Michael Shaffer, Department of Geological Sciences, University of Oregon, Eugene; (b) courtesy of Dr. J. M. Hudak, McMaster University, Hamilton, Ontario, Canada.)

can achieve magnification of 10,000× or more. Figure 1.21 shows two SEM images of specimen failures due to thermal overload.

We conclude the discussion of imaging modalities by looking briefly at images that are not obtained from physical objects. Instead, they are generated by computer. *Fractals* are striking examples of computer-generated images (Lu [1997]). Basically, a fractal is nothing more than an iterative reproduction of a basic pattern according to some mathematical rules. For instance, *tiling* is one of the simplest ways to generate a fractal image. A square can be subdivided into four square subregions, each of which can be further subdivided into four smaller square regions, and so on. Depending on the complexity of the rules for filling each subsquare, some beautiful tile images can be generated using this method. Of course, the geometry can be arbitrary. For instance, the fractal image could be grown radially out of a center point. Figure 1.22(a) shows a fractal grown in this way. Figure 1.22(b) shows another fractal (a "moonscape") that provides an interesting analogy to the images of space used as illustrations in some of the preceding sections.

Fractal images tend toward artistic, mathematical formulations of "growth" of subimage elements according to a set of rules. They are useful sometimes as random textures. A more structured approach to image generation by computer lies in 3-D modeling. This is an area that provides an important intersection between image processing and computer graphics and is the basis for many 3-D visualization systems (e.g., flight simulators). Figures 1.22(c) and (d) show examples of computer-generated images. Since the original object is created in 3-D, images can be generated in any perspective from plane projections of the 3-D volume. Images of this type can be used for medical training and for a host of other applications, such as criminal forensics and special effects.

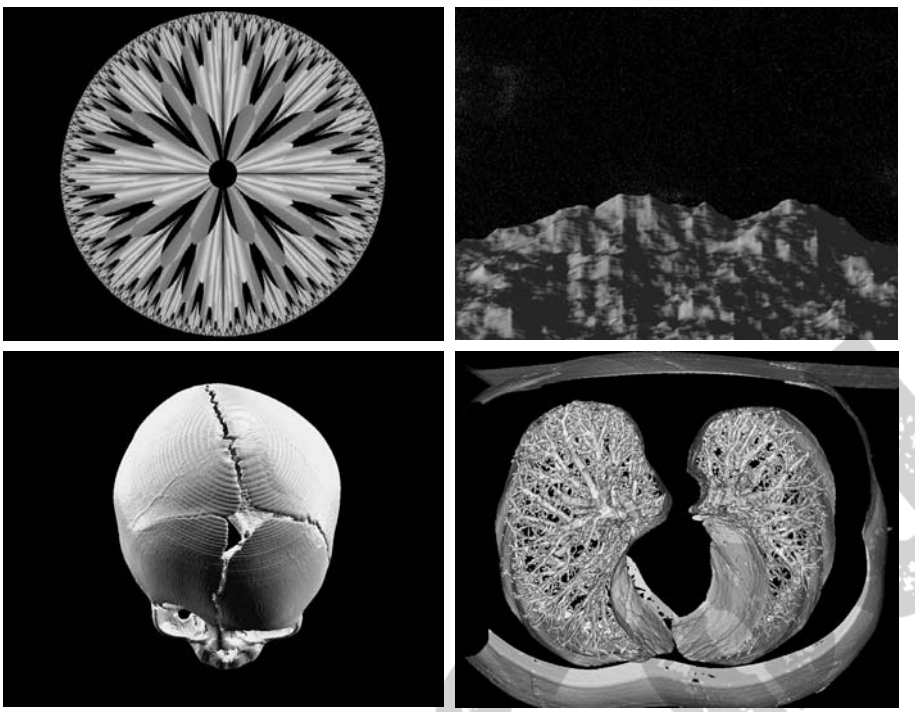

a b
c d

FIGURE 1.22
(a) and (b) Fractal images. (c) and (d) Images generated from 3-D computer models of the objects shown. (Figures (a) and (b) courtesy of Ms. Melissa D. Binde, Swarthmore College; (c) and (d) courtesy of NASA.)

1.4 Fundamental Steps in Digital Image Processing

It is helpful to divide the material covered in the following chapters into the two broad categories defined in Section 1.1: methods whose input and output are images, and methods whose inputs may be images but whose outputs are attributes extracted from those images. This organization is summarized in Fig. 1.23. The diagram does not imply that every process is applied to an image. Rather, the intention is to convey an idea of all the methodologies that can be applied to images for different purposes and possibly with different objectives. The discussion in this section may be viewed as a brief overview of the material in the remainder of the book.

Image acquisition is the first process in Fig. 1.23. The discussion in Section 1.3 gave some hints regarding the origin of digital images. This topic is considered in much more detail in Chapter 2, where we also introduce a number of basic digital image concepts that are used throughout the book. Note that acquisition could be as simple as being given an image that is already in digital form. Generally, the image acquisition stage involves preprocessing, such as scaling.

Image enhancement is the process of manipulating an image so that the result is more suitable than the original for a specific application. The word *specific* is important here, because it establishes at the outset that enhancement techniques are problem oriented. Thus, for example, a method that is quite useful for enhancing X-ray images may not be the best approach for enhancing satellite images taken in the infrared band of the electromagnetic spectrum.

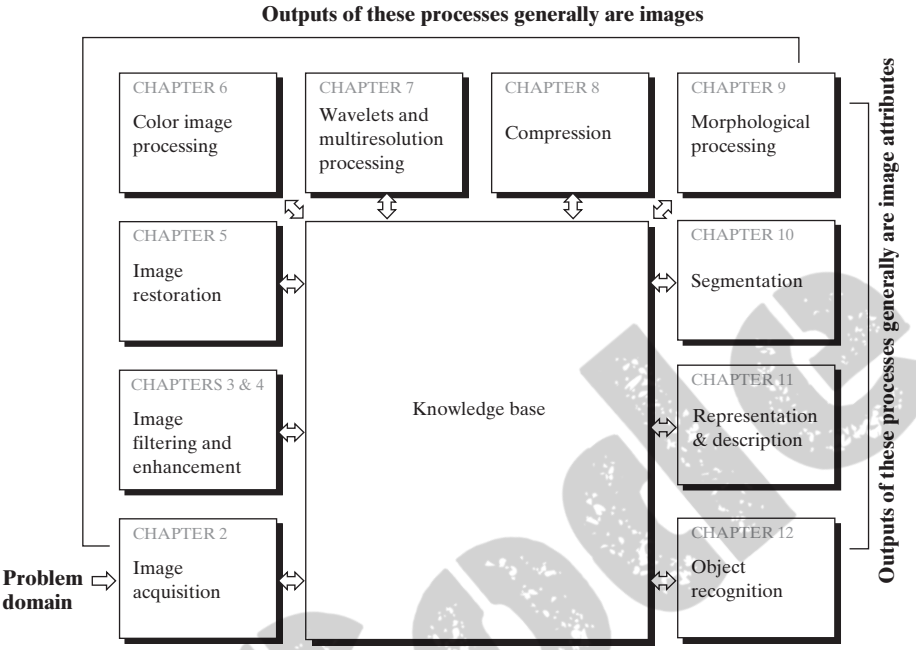

FIGURE 1.23 Fundamental steps in digital image processing. The chapter(s) indicated in the boxes is where the material described in the box is discussed.

There is no general "theory" of image enhancement. When an image is processed for visual interpretation, the viewer is the ultimate judge of how well a particular method works. Enhancement techniques are so varied, and use so many different image processing approaches, that it is difficult to assemble a meaningful body of techniques suitable for enhancement in one chapter without extensive background development. For this reason, and also because beginners in the field of image processing generally find enhancement applications visually appealing, interesting, and relatively simple to understand, we use image enhancement as examples when introducing new concepts in parts of Chapter 2 and in Chapters 3 and 4. The material in the latter two chapters span many of the methods used traditionally for image enhancement. Therefore, using examples from image enhancement to introduce new image processing methods developed in these early chapters not only saves having an extra chapter in the book dealing with image enhancement but, more importantly, is an effective approach for introducing newcomers to the details of processing techniques early in the book. However, as you will see in progressing through the rest of the book, the material developed in these chapters is applicable to a much broader class of problems than just image enhancement.

Image restoration is an area that also deals with improving the appearance of an image. However, unlike enhancement, which is subjective, image restoration is objective, in the sense that restoration techniques tend to be based on mathematical or probabilistic models of image degradation. Enhancement, on the other hand, is based on human subjective preferences regarding what constitutes a "good" enhancement result.

Color image processing is an area that has been gaining in importance because of the significant increase in the use of digital images over the Internet. Chapter 6 covers a number of fundamental concepts in color models and basic color processing in a digital domain. Color is used also in later chapters as the basis for extracting features of interest in an image.

Wavelets are the foundation for representing images in various degrees of resolution. In particular, this material is used in this book for image data compression and for pyramidal representation, in which images are subdivided successively into smaller regions.

Compression, as the name implies, deals with techniques for reducing the storage required to save an image, or the bandwidth required to transmit it. Although storage technology has improved significantly over the past decade, the same cannot be said for transmission capacity. This is true particularly in uses of the Internet, which are characterized by significant pictorial content. Image compression is familiar (perhaps inadvertently) to most users of computers in the form of image file extensions, such as the jpg file extension used in the JPEG (Joint Photographic Experts Group) image compression standard.

Morphological processing deals with tools for extracting image components that are useful in the representation and description of shape. The material in this chapter begins a transition from processes that output images to processes that output image attributes, as indicated in Section 1.1.

Segmentation procedures partition an image into its constituent parts or objects. In general, autonomous segmentation is one of the most difficult tasks in digital image processing. A rugged segmentation procedure brings the process a long way toward successful solution of imaging problems that require objects to be identified individually. On the other hand, weak or erratic segmentation algorithms almost always guarantee eventual failure. In general, the more accurate the segmentation, the more likely recognition is to succeed.

Representation and description almost always follow the output of a segmentation stage, which usually is raw pixel data, constituting either the boundary of a region (i.e., the set of pixels separating one image region from another) or all the points in the region itself. In either case, converting the data to a form suitable for computer processing is necessary. The first decision that must be made is whether the data should be represented as a boundary or as a complete region. Boundary representation is appropriate when the focus is on external shape characteristics, such as corners and inflections. Regional representation is appropriate when the focus is on internal properties, such as texture or skeletal shape. In some applications, these representations complement each other. Choosing a representation is only part of the solution for transforming raw data into a form suitable for subsequent computer processing. A method must also be specified for describing the data so that features of interest are highlighted. *Description*, also called *feature selection*, deals with extracting attributes that result in some quantitative information of interest or are basic for differentiating one class of objects from another.

Recognition is the process that assigns a label (e.g., "vehicle") to an object based on its descriptors. As detailed in Section 1.1, we conclude our coverage of

digital image processing with the development of methods for recognition of individual objects.

So far we have said nothing about the need for prior knowledge or about the interaction between the *knowledge base* and the processing modules in Fig. 1.23. Knowledge about a problem domain is coded into an image processing system in the form of a knowledge database. This knowledge may be as simple as detailing regions of an image where the information of interest is known to be located, thus limiting the search that has to be conducted in seeking that information. The knowledge base also can be quite complex, such as an interrelated list of all major possible defects in a materials inspection problem or an image database containing high-resolution satellite images of a region in connection with change-detection applications. In addition to guiding the operation of each processing module, the knowledge base also controls the interaction between modules. This distinction is made in Fig. 1.23 by the use of double-headed arrows between the processing modules and the knowledge base, as opposed to single-headed arrows linking the processing modules.

Although we do not discuss image display explicitly at this point, it is important to keep in mind that viewing the results of image processing can take place at the output of any stage in Fig. 1.23. We also note that not all image processing applications require the complexity of interactions implied by Fig. 1.23. In fact, not even all those modules are needed in many cases. For example, image enhancement for human visual interpretation seldom requires use of any of the other stages in Fig. 1.23. In general, however, as the complexity of an image processing task increases, so does the number of processes required to solve the problem.

1.5 Components of an Image Processing System

As recently as the mid-1980s, numerous models of image processing systems being sold throughout the world were rather substantial peripheral devices that attached to equally substantial host computers. Late in the 1980s and early in the 1990s, the market shifted to image processing hardware in the form of single boards designed to be compatible with industry standard buses and to fit into engineering workstation cabinets and personal computers. In addition to lowering costs, this market shift also served as a catalyst for a significant number of new companies specializing in the development of software written specifically for image processing.

Although large-scale image processing systems still are being sold for massive imaging applications, such as processing of satellite images, the trend continues toward miniaturizing and blending of general-purpose small computers with specialized image processing hardware. Figure 1.24 shows the basic components comprising a typical *general-purpose* system used for digital image processing. The function of each component is discussed in the following paragraphs, starting with image sensing.

With reference to *sensing*, two elements are required to acquire digital images. The first is a physical device that is sensitive to the energy radiated by the object we wish to image. The second, called a *digitizer*, is a device for converting

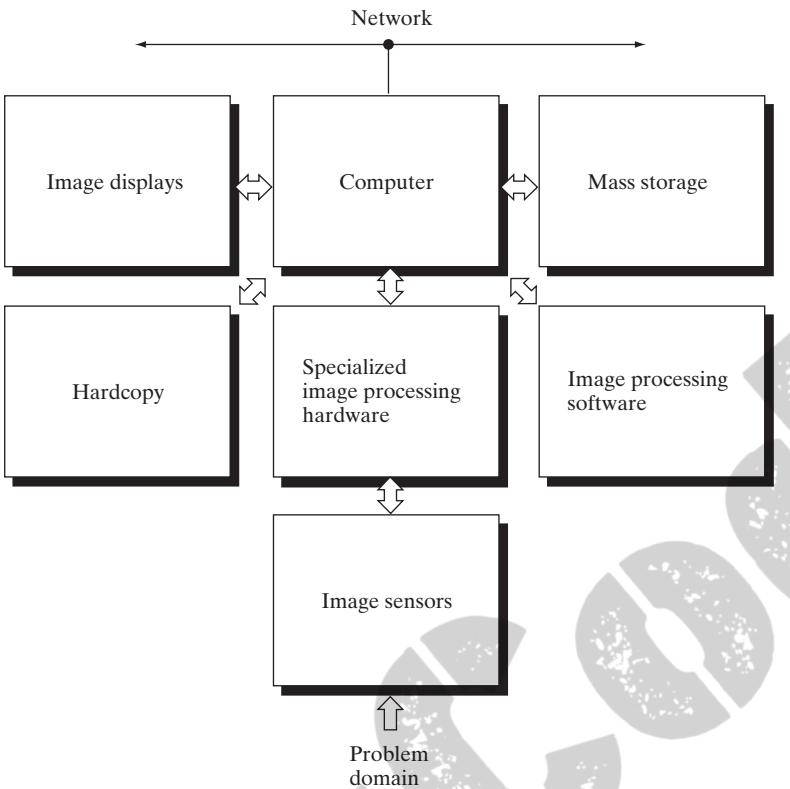

FIGURE 1.24 Components of a general-purpose image processing system.

the output of the physical sensing device into digital form. For instance, in a digital video camera, the sensors produce an electrical output proportional to light intensity. The digitizer converts these outputs to digital data. These topics are covered in Chapter 2.

Specialized image processing hardware usually consists of the digitizer just mentioned, plus hardware that performs other primitive operations, such as an arithmetic logic unit (ALU), that performs arithmetic and logical operations in parallel on entire images. One example of how an ALU is used is in averaging images as quickly as they are digitized, for the purpose of noise reduction. This type of hardware sometimes is called a *front-end subsystem*, and its most distinguishing characteristic is speed. In other words, this unit performs functions that require fast data throughputs (e.g., digitizing and averaging video images at 30 frames/s) that the typical main computer cannot handle.

The *computer* in an image processing system is a general-purpose computer and can range from a PC to a supercomputer. In dedicated applications, sometimes custom computers are used to achieve a required level of performance, but our interest here is on general-purpose image processing systems. In these systems, almost any well-equipped PC-type machine is suitable for off-line image processing tasks.

Software for image processing consists of specialized modules that perform specific tasks. A well-designed package also includes the capability for the user

to write code that, as a minimum, utilizes the specialized modules. More sophisticated software packages allow the integration of those modules and general-purpose software commands from at least one computer language.

Mass storage capability is a must in image processing applications. An image of size 1024×1024 pixels, in which the intensity of each pixel is an 8-bit quantity, requires one megabyte of storage space if the image is not compressed. When dealing with thousands, or even millions, of images, providing adequate storage in an image processing system can be a challenge. Digital storage for image processing applications falls into three principal categories: (1) short-term storage for use during processing, (2) on-line storage for relatively fast recall, and (3) archival storage, characterized by infrequent access. Storage is measured in bytes (eight bits), Kbytes (one thousand bytes), Mbytes (one million bytes), Gbytes (meaning giga, or one billion, bytes), and Tbytes (meaning tera, or one trillion, bytes).

One method of providing short-term storage is computer memory. Another is by specialized boards, called *frame buffers*, that store one or more images and can be accessed rapidly, usually at video rates (e.g., at 30 complete images per second). The latter method allows virtually instantaneous image *zoom*, as well as *scroll* (vertical shifts) and *pan* (horizontal shifts). Frame buffers usually are housed in the specialized image processing hardware unit in Fig. 1.24. On-line storage generally takes the form of magnetic disks or optical-media storage. The key factor characterizing on-line storage is frequent access to the stored data. Finally, archival storage is characterized by massive storage requirements but infrequent need for access. Magnetic tapes and optical disks housed in "jukeboxes" are the usual media for archival applications.

Image displays in use today are mainly color (preferably flat screen) TV monitors. Monitors are driven by the outputs of image and graphics display cards that are an integral part of the computer system. Seldom are there requirements for image display applications that cannot be met by display cards available commercially as part of the computer system. In some cases, it is necessary to have stereo displays, and these are implemented in the form of headgear containing two small displays embedded in goggles worn by the user.

Hardcopy devices for recording images include laser printers, film cameras, heat-sensitive devices, inkjet units, and digital units, such as optical and CD-ROM disks. Film provides the highest possible resolution, but paper is the obvious medium of choice for written material. For presentations, images are displayed on film transparencies or in a digital medium if image projection equipment is used. The latter approach is gaining acceptance as the standard for image presentations.

Networking is almost a default function in any computer system in use today. Because of the large amount of data inherent in image processing applications, the key consideration in image transmission is bandwidth. In dedicated networks, this typically is not a problem, but communications with remote sites via the Internet are not always as efficient. Fortunately, this situation is improving quickly as a result of optical fiber and other broadband technologies.

2.1 Elements of Visual Perception

Although the field of digital image processing is built on a foundation of mathematical and probabilistic formulations, human intuition and analysis play a central role in the choice of one technique versus another, and this choice often is made based on subjective, visual judgments. Hence, developing a basic understanding of human visual perception as a first step in our journey through this book is appropriate. Given the complexity and breadth of this topic, we can only aspire to cover the most rudimentary aspects of human vision. In particular, our interest is in the mechanics and parameters related to how images are formed and perceived by humans. We are interested in learning the physical limitations of human vision in terms of factors that also are used in our work with digital images. Thus, factors such as how human and electronic imaging devices compare in terms of resolution and ability to adapt to changes in illumination are not only interesting, they also are important from a practical point of view.

2.1.1 Structure of the Human Eye

Figure 2.1 shows a simplified horizontal cross section of the human eye. The eye is nearly a sphere, with an average diameter of approximately 20 mm. Three membranes enclose the eye: the *cornea* and *sclera* outer cover; the *choroid*; and the *retina*. The cornea is a tough, transparent tissue that covers

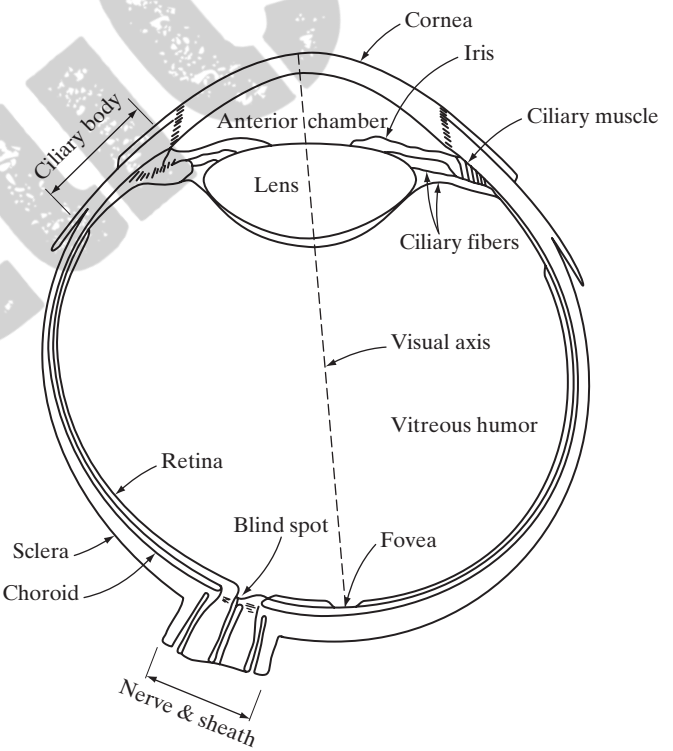

FIGURE 2.1 Simplified diagram of a cross section of the human eye.

the anterior surface of the eye. Continuous with the cornea, the sclera is an opaque membrane that encloses the remainder of the optic globe.

The choroid lies directly below the sclera. This membrane contains a network of blood vessels that serve as the major source of nutrition to the eye. Even superficial injury to the choroid, often not deemed serious, can lead to severe eye damage as a result of inflammation that restricts blood flow. The choroid coat is heavily pigmented and hence helps to reduce the amount of extraneous light entering the eye and the backscatter within the optic globe. At its anterior extreme, the choroid is divided into the *ciliary body* and the *iris*. The latter contracts or expands to control the amount of light that enters the eye. The central opening of the iris (the pupil) varies in diameter from approximately 2 to 8 mm. The front of the iris contains the visible pigment of the eye, whereas the back contains a black pigment.

The *lens* is made up of concentric layers of fibrous cells and is suspended by fibers that attach to the ciliary body. It contains 60 to 70% water, about 6% fat, and more protein than any other tissue in the eye. The lens is colored by a slightly yellow pigmentation that increases with age. In extreme cases, excessive clouding of the lens, caused by the affliction commonly referred to as *cataracts*, can lead to poor color discrimination and loss of clear vision. The lens absorbs approximately 8% of the visible light spectrum, with relatively higher absorption at shorter wavelengths. Both infrared and ultraviolet light are absorbed appreciably by proteins within the lens structure and, in excessive amounts, can damage the eye.

The innermost membrane of the eye is the *retina*, which lines the inside of the wall's entire posterior portion. When the eye is properly focused, light from an object outside the eye is imaged on the retina. Pattern vision is afforded by the distribution of discrete light receptors over the surface of the retina. There are two classes of receptors: *cones* and *rods*. The cones in each eye number between 6 and 7 million. They are located primarily in the central portion of the retina, called the *fovea*, and are highly sensitive to color. Humans can resolve fine details with these cones largely because each one is connected to its own nerve end. Muscles controlling the eye rotate the eyeball until the image of an object of interest falls on the fovea. Cone vision is called *photopic* or bright-light vision.

The number of rods is much larger: Some 75 to 150 million are distributed over the retinal surface. The larger area of distribution and the fact that several rods are connected to a single nerve end reduce the amount of detail discernible by these receptors. Rods serve to give a general, overall picture of the field of view. They are not involved in color vision and are sensitive to low levels of illumination. For example, objects that appear brightly colored in daylight when seen by moonlight appear as colorless forms because only the rods are stimulated. This phenomenon is known as *scotopic* or dim-light vision.

Figure 2.2 shows the density of rods and cones for a cross section of the right eye passing through the region of emergence of the optic nerve from the eye. The absence of receptors in this area results in the so-called *blind spot* (see Fig. 2.1). Except for this region, the distribution of receptors is radially symmetric about the fovea. Receptor density is measured in degrees from the

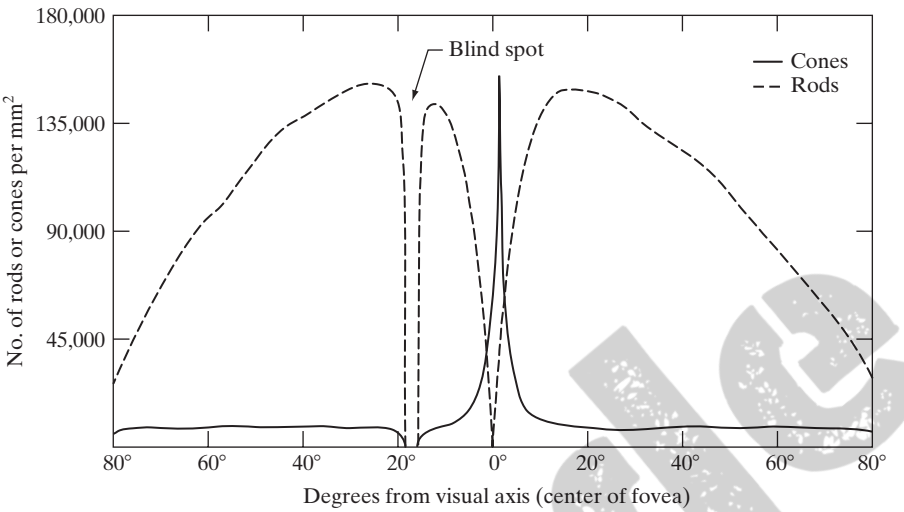

FIGURE 2.2 Distribution of rods and cones in the retina.

fovea (that is, in degrees off axis, as measured by the angle formed by the visual axis and a line passing through the center of the lens and intersecting the retina). Note in Fig. 2.2 that cones are most dense in the center of the retina (in the center area of the fovea). Note also that rods increase in density from the center out to approximately 20° off axis and then decrease in density out to the extreme periphery of the retina.

The fovea itself is a circular indentation in the retina of about 1.5 mm in diameter. However, in terms of future discussions, talking about square or rectangular arrays of sensing elements is more useful. Thus, by taking some liberty in interpretation, we can view the fovea as a square sensor array of size 1.5 mm $\times$ 1.5 mm. The density of cones in that area of the retina is approximately 150,000 elements per mm^2. Based on these approximations, the number of cones in the region of highest acuity in the eye is about 337,000 elements. Just in terms of raw resolving power, a charge-coupled device (CCD) imaging chip of medium resolution can have this number of elements in a receptor array no larger than 5 mm $\times$ 5 mm. While the ability of humans to integrate intelligence and experience with vision makes these types of number comparisons somewhat superficial, keep in mind for future discussions that the basic ability of the eye to resolve detail certainly is comparable to current electronic imaging sensors.

2.1.2 Image Formation in the Eye

In an ordinary photographic camera, the lens has a fixed focal length, and focusing at various distances is achieved by varying the distance between the lens and the imaging plane, where the film (or imaging chip in the case of a digital camera) is located. In the human eye, the converse is true; the distance between the lens and the imaging region (the retina) is fixed, and the focal length needed to achieve proper focus is obtained by varying the shape of the lens. The fibers in the ciliary body accomplish this, flattening or thickening the

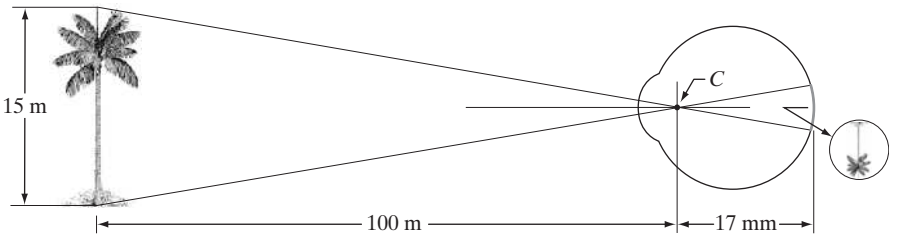

FIGURE 2.3 Graphical representation of the eye looking at a palm tree. Point *C* is the optical center of the lens.

lens for distant or near objects, respectively. The distance between the center of the lens and the retina along the visual axis is approximately 17 mm. The range of focal lengths is approximately 14 mm to 17 mm, the latter taking place when the eye is relaxed and focused at distances greater than about 3 m.

The geometry in Fig. 2.3 illustrates how to obtain the dimensions of an image formed on the retina. For example, suppose that a person is looking at a tree 15 m high at a distance of 100 m. Letting h denote the height of that object in the retinal image, the geometry of Fig. 2.3 yields $15/100 = h/17$ or $h = 2.55$ mm. As indicated in Section 2.1.1, the retinal image is focused primarily on the region of the fovea. Perception then takes place by the relative excitation of light receptors, which transform radiant energy into electrical impulses that ultimately are decoded by the brain.

2.1.3 Brightness Adaptation and Discrimination

Because digital images are displayed as a discrete set of intensities, the eye's ability to discriminate between different intensity levels is an important consideration in presenting image processing results. The range of light intensity levels to which the human visual system can adapt is enormous—on the order of 10^{10}—from the scotopic threshold to the glare limit. Experimental evidence indicates that *subjective brightness* (intensity as *perceived* by the human visual system) is a logarithmic function of the light intensity incident on the eye. Figure 2.4, a plot

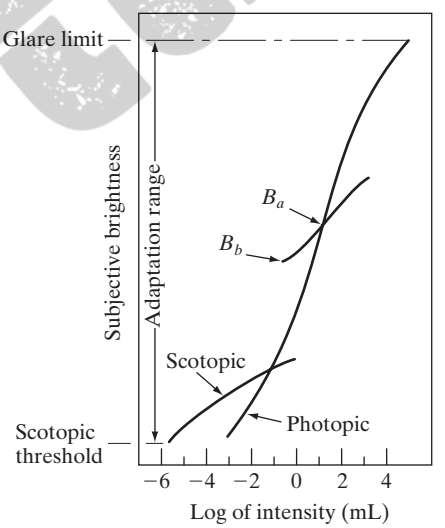

FIGURE 2.4 Range of subjective brightness sensations showing a particular adaptation level.

of light intensity versus subjective brightness, illustrates this characteristic. The long solid curve represents the range of intensities to which the visual system can adapt. In photopic vision alone, the range is about 10^6. The transition from scotopic to photopic vision is gradual over the approximate range from 0.001 to 0.1 millilambert (−3 to −1 mL in the log scale), as the double branches of the adaptation curve in this range show.

The essential point in interpreting the impressive dynamic range depicted in Fig. 2.4 is that the visual system cannot operate over such a range *simultaneously.* Rather, it accomplishes this large variation by changing its overall sensitivity, a phenomenon known as *brightness adaptation.* The total range of distinct intensity levels the eye can discriminate simultaneously is rather small when compared with the total adaptation range. For any given set of conditions, the current sensitivity level of the visual system is called the *brightness adaptation level,* which may correspond, for example, to brightness B_a in Fig. 2.4. The short intersecting curve represents the range of subjective brightness that the eye can perceive when adapted to this level. This range is rather restricted, having a level B_b at and below which all stimuli are perceived as indistinguishable blacks. The upper portion of the curve is not actually restricted but, if extended too far, loses its meaning because much higher intensities would simply raise the adaptation level higher than B_a.

The ability of the eye to discriminate between *changes* in light intensity at any specific adaptation level is also of considerable interest. A classic experiment used to determine the capability of the human visual system for brightness discrimination consists of having a subject look at a flat, uniformly illuminated area large enough to occupy the entire field of view. This area typically is a diffuser, such as opaque glass, that is illuminated from behind by a light source whose intensity, I, can be varied. To this field is added an increment of illumination, ΔI, in the form of a short-duration flash that appears as a circle in the center of the uniformly illuminated field, as Fig. 2.5 shows.

If ΔI is not bright enough, the subject says "no," indicating no perceivable change. As ΔI gets stronger, the subject may give a positive response of "yes," indicating a perceived change. Finally, when ΔI is strong enough, the subject will give a response of "yes" all the time. The quantity $\Delta I_c/I$, where ΔI_c is the increment of illumination discriminable 50% of the time with background illumination I, is called the *Weber ratio*. A small value of $\Delta I_c/I$ means that a small percentage change in intensity is discriminable. This represents "good" brightness discrimination. Conversely, a large value of $\Delta I_c/I$ means that a large percentage change in intensity is required. This represents "poor" brightness discrimination.

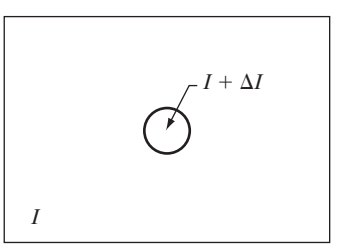

FIGURE 2.5 Basic experimental setup used to characterize brightness discrimination.

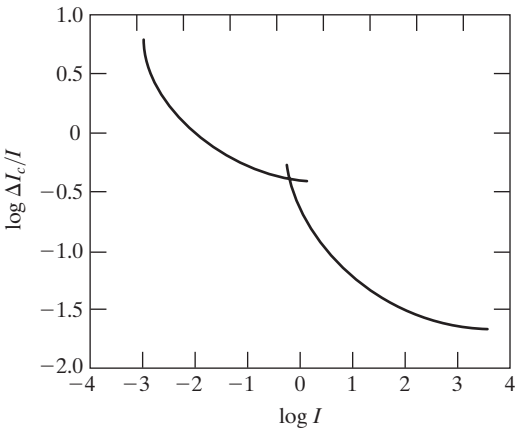

FIGURE 2.6
Typical Weber ratio as a function of intensity.

A plot of log $\Delta I_c/I$ as a function of log I has the general shape shown in Fig. 2.6. This curve shows that brightness discrimination is poor (the Weber ratio is large) at low levels of illumination, and it improves significantly (the Weber ratio decreases) as background illumination increases. The two branches in the curve reflect the fact that at low levels of illumination vision is carried out by the rods, whereas at high levels (showing better discrimination) vision is the function of cones.

If the background illumination is held constant and the intensity of the other source, instead of flashing, is now allowed to vary incrementally from never being perceived to always being perceived, the typical observer can discern a total of one to two dozen different intensity changes. Roughly, this result is related to the number of different intensities a person can see at any one point in a monochrome image. This result does not mean that an image can be represented by such a small number of intensity values because, as the eye roams about the image, the average background changes, thus allowing a *different* set of incremental changes to be detected at each new adaptation level. The net consequence is that the eye is capable of a much broader range of *overall* intensity discrimination. In fact, we show in Section 2.4.3 that the eye is capable of detecting objectionable contouring effects in monochrome images whose overall intensity is represented by fewer than approximately two dozen levels.

Two phenomena clearly demonstrate that perceived brightness is not a simple function of intensity. The first is based on the fact that the visual system tends to undershoot or overshoot around the boundary of regions of different intensities. Figure 2.7(a) shows a striking example of this phenomenon. Although the intensity of the stripes is constant, we actually perceive a brightness pattern that is strongly scalloped near the boundaries [Fig. 2.7(c)]. These seemingly scalloped bands are called *Mach bands* after Ernst Mach, who first described the phenomenon in 1865.

The second phenomenon, called *simultaneous contrast*, is related to the fact that a region's perceived brightness does not depend simply on its intensity, as Fig. 2.8 demonstrates. All the center squares have exactly the same intensity.

a
b
c

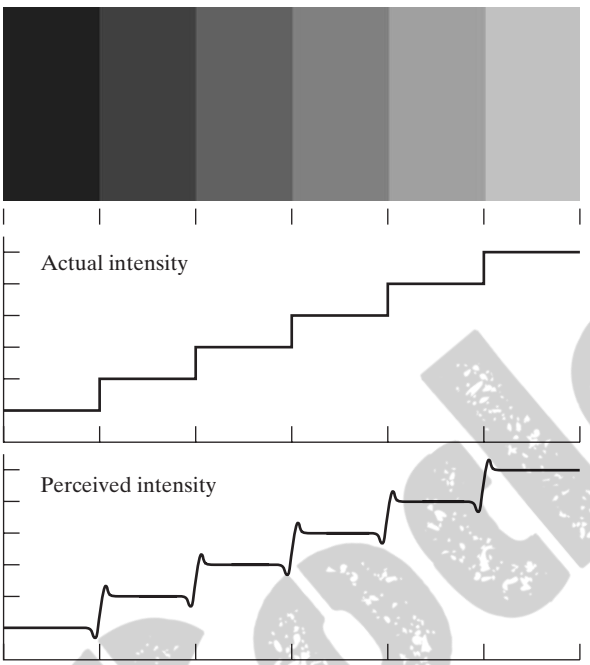

FIGURE 2.7 Illustration of the Mach band effect. Perceived intensity is not a simple function of actual intensity.

However, they appear to the eye to become darker as the background gets lighter. A more familiar example is a piece of paper that seems white when lying on a desk, but can appear totally black when used to shield the eyes while looking directly at a bright sky.

Other examples of human perception phenomena are optical illusions, in which the eye fills in nonexisting information or wrongly perceives geometrical properties of objects. Figure 2.9 shows some examples. In Fig. 2.9(a), the outline of a square is seen clearly, despite the fact that no lines defining such a figure are part of the image. The same effect, this time with a circle, can be seen in Fig. 2.9(b); note how just a few lines are sufficient to give the illusion of a

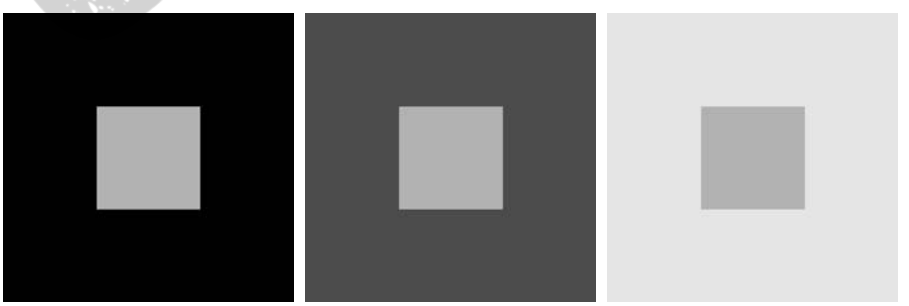

a b c

FIGURE 2.8 Examples of simultaneous contrast. All the inner squares have the same intensity, but they appear progressively darker as the background becomes lighter.

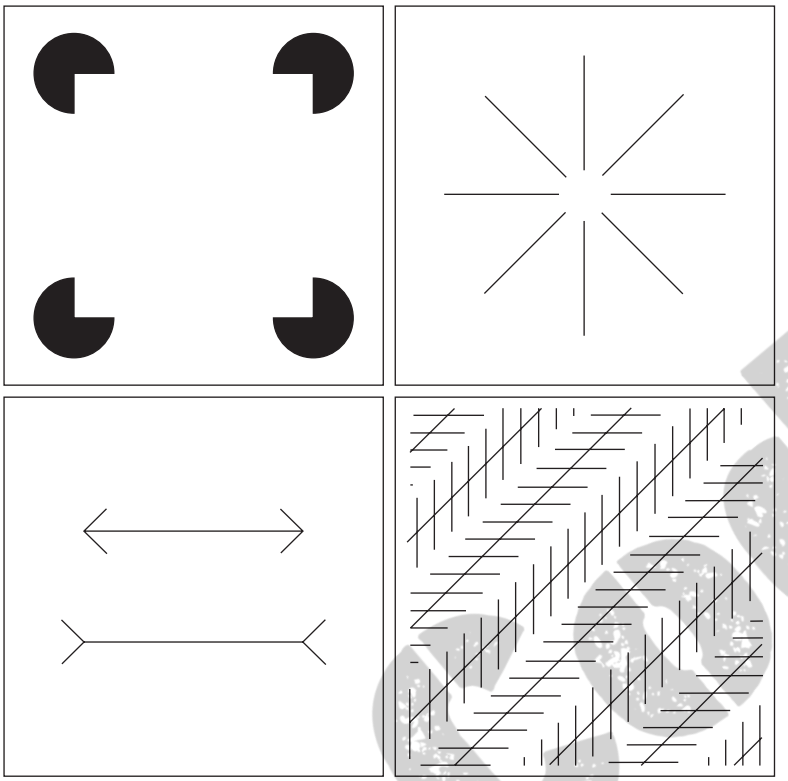

a b
c d

FIGURE 2.9 Some well-known optical illusions.

complete circle. The two horizontal line segments in Fig. 2.9(c) are of the same length, but one appears shorter than the other. Finally, all lines in Fig. 2.9(d) that are oriented at 45° are equidistant and parallel. Yet the crosshatching creates the illusion that those lines are far from being parallel. Optical illusions are a characteristic of the human visual system that is not fully understood.

2.2 Light and the Electromagnetic Spectrum

The electromagnetic spectrum was introduced in Section 1.3. We now consider this topic in more detail. In 1666, Sir Isaac Newton discovered that when a beam of sunlight is passed through a glass prism, the emerging beam of light is not white but consists instead of a continuous spectrum of colors ranging from violet at one end to red at the other. As Fig. 2.10 shows, the range of colors we perceive in visible light represents a very small portion of the electromagnetic spectrum. On one end of the spectrum are radio waves with wavelengths billions of times longer than those of visible light. On the other end of the spectrum are gamma rays with wavelengths millions of times smaller than those of visible light. The electromagnetic spectrum can be expressed in terms of wavelength, frequency, or energy. Wavelength (λ) and frequency (ν) are related by the expression

$$\lambda = \frac{c}{\nu} \tag{2.2-1}$$

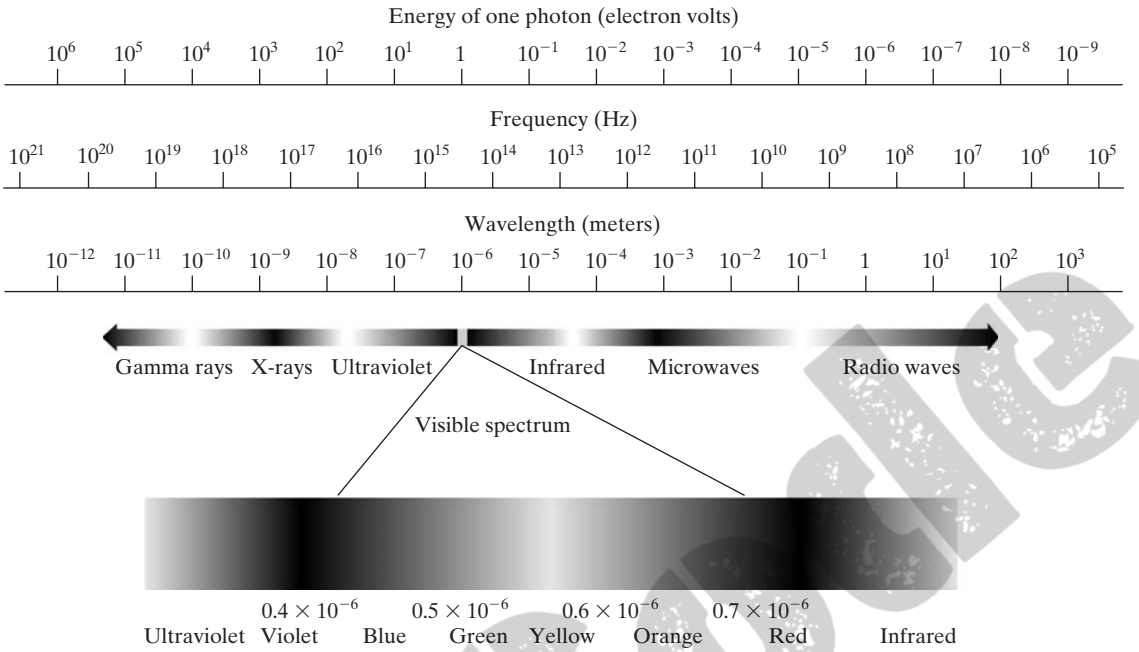

FIGURE 2.10 The electromagnetic spectrum. The visible spectrum is shown zoomed to facilitate explanation, but note that the visible spectrum is a rather narrow portion of the EM spectrum.

where c is the speed of light (2.998×10^8 m/s). The energy of the various components of the electromagnetic spectrum is given by the expression

$$E = h\nu \tag{2.2-2}$$

where h is Planck's constant. The units of wavelength are meters, with the terms *microns* (denoted μm and equal to 10^{-6} m) and *nanometers* (denoted nm and equal to 10^{-9} m) being used just as frequently. Frequency is measured in Hertz (Hz), with one Hertz being equal to one cycle of a sinusoidal wave per second. A commonly used unit of energy is the electron-volt.

Electromagnetic waves can be visualized as propagating sinusoidal waves with wavelength λ (Fig. 2.11), or they can be thought of as a stream of massless particles, each traveling in a wavelike pattern and moving at the speed of light. Each massless particle contains a certain amount (or bundle) of energy. Each

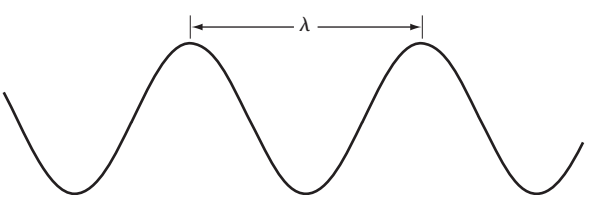

FIGURE 2.11 Graphical representation of one wavelength.

bundle of energy is called a *photon*. We see from Eq. (2.2-2) that energy is proportional to frequency, so the higher-frequency (shorter wavelength) electromagnetic phenomena carry more energy per photon. Thus, radio waves have photons with low energies, microwaves have more energy than radio waves, infrared still more, then visible, ultraviolet, X-rays, and finally gamma rays, the most energetic of all. This is the reason why gamma rays are so dangerous to living organisms.

Light is a particular type of electromagnetic radiation that can be sensed by the human eye. The visible (color) spectrum is shown expanded in Fig. 2.10 for the purpose of discussion (we consider color in much more detail in Chapter 6). The visible band of the electromagnetic spectrum spans the range from approximately 0.43 μm (violet) to about 0.79 μm (red). For convenience, the color spectrum is divided into six broad regions: violet, blue, green, yellow, orange, and red. No color (or other component of the electromagnetic spectrum) ends abruptly, but rather each range blends smoothly into the next, as shown in Fig. 2.10.

The colors that humans perceive in an object are determined by the nature of the light *reflected* from the object. A body that reflects light relatively balanced in all visible wavelengths appears white to the observer. However, a body that favors reflectance in a limited range of the visible spectrum exhibits some shades of color. For example, green objects reflect light with wavelengths primarily in the 500 to 570 nm range while absorbing most of the energy at other wavelengths.

Light that is void of color is called *monochromatic* (or *achromatic*) *light*. The only attribute of monochromatic light is its *intensity* or amount. Because the intensity of monochromatic light is perceived to vary from black to grays and finally to white, the term *gray level* is used commonly to denote monochromatic intensity. We use the terms *intensity* and *gray level* interchangeably in subsequent discussions. The range of measured values of monochromatic light from black to white is usually called the *gray scale*, and monochromatic images are frequently referred to as *gray-scale images*.

Chromatic (*color*) *light* spans the electromagnetic energy spectrum from approximately 0.43 to 0.79 μm, as noted previously. In addition to frequency, three basic quantities are used to describe the quality of a chromatic light source: radiance, luminance, and brightness. *Radiance* is the total amount of energy that flows from the light source, and it is usually measured in watts (W). *Luminance*, measured in lumens (lm), gives a measure of the amount of energy an observer *perceives* from a light source. For example, light emitted from a source operating in the far infrared region of the spectrum could have significant energy (radiance), but an observer would hardly perceive it; its luminance would be almost zero. Finally, as discussed in Section 2.1, *brightness* is a subjective descriptor of light perception that is practically impossible to measure. It embodies the achromatic notion of intensity and is one of the key factors in describing color sensation.

Continuing with the discussion of Fig. 2.10, we note that at the short-wavelength end of the electromagnetic spectrum, we have gamma rays and X-rays. As discussed in Section 1.3.1, gamma radiation is important for medical and astronomical imaging, and for imaging radiation in nuclear environments.

Hard (high-energy) X-rays are used in industrial applications. Chest and dental X-rays are in the lower energy (soft) end of the X-ray band. The soft X-ray band transitions into the far ultraviolet light region, which in turn blends with the visible spectrum at longer wavelengths. Moving still higher in wavelength, we encounter the infrared band, which radiates heat, a fact that makes it useful in imaging applications that rely on "heat signatures." The part of the infrared band close to the visible spectrum is called the *near-infrared* region. The opposite end of this band is called the *far-infrared* region. This latter region blends with the microwave band. This band is well known as the source of energy in microwave ovens, but it has many other uses, including communication and radar. Finally, the radio wave band encompasses television as well as AM and FM radio. In the higher energies, radio signals emanating from certain stellar bodies are useful in astronomical observations. Examples of images in most of the bands just discussed are given in Section 1.3.

In principle, if a sensor can be developed that is capable of detecting energy radiated by a band of the electromagnetic spectrum, we can image events of interest in that band. It is important to note, however, that the wavelength of an electromagnetic wave required to "see" an object must be of the same size as or smaller than the object. For example, a water molecule has a diameter on the order of 10^{-10} m. Thus, to study molecules, we would need a source capable of emitting in the far ultraviolet or soft X-ray region. This limitation, along with the physical properties of the sensor material, establishes the fundamental limits on the capability of imaging sensors, such as visible, infrared, and other sensors in use today.

Although imaging is based predominantly on energy radiated by electromagnetic waves, this is not the only method for image generation. For example, as discussed in Section 1.3.7, sound reflected from objects can be used to form ultrasonic images. Other major sources of digital images are electron beams for electron microscopy and synthetic images used in graphics and visualization.

2.3 Image Sensing and Acquisition

Most of the images in which we are interested are generated by the combination of an "illumination" source and the reflection or absorption of energy from that source by the elements of the "scene" being imaged. We enclose *illumination* and *scene* in quotes to emphasize the fact that they are considerably more general than the familiar situation in which a visible light source illuminates a common everyday 3-D (three-dimensional) scene. For example, the illumination may originate from a source of electromagnetic energy such as radar, infrared, or X-ray system. But, as noted earlier, it could originate from less traditional sources, such as ultrasound or even a computer-generated illumination pattern. Similarly, the scene elements could be familiar objects, but they can just as easily be molecules, buried rock formations, or a human brain. Depending on the nature of the source, illumination energy is reflected from, or transmitted through, objects. An example in the first category is light

reflected from a planar surface. An example in the second category is when X-rays pass through a patient's body for the purpose of generating a diagnostic X-ray film. In some applications, the reflected or transmitted energy is focused onto a photoconverter (e.g., a phosphor screen), which converts the energy into visible light. Electron microscopy and some applications of gamma imaging use this approach.

Figure 2.12 shows the three principal sensor arrangements used to transform illumination energy into digital images. The idea is simple: Incoming energy is transformed into a voltage by the combination of input electrical power and sensor material that is responsive to the particular type of energy being detected. The output voltage waveform is the response of the sensor(s), and a digital quantity is obtained from each sensor by digitizing its response. In this section, we look at the principal modalities for image sensing and generation. Image digitizing is discussed in Section 2.4.

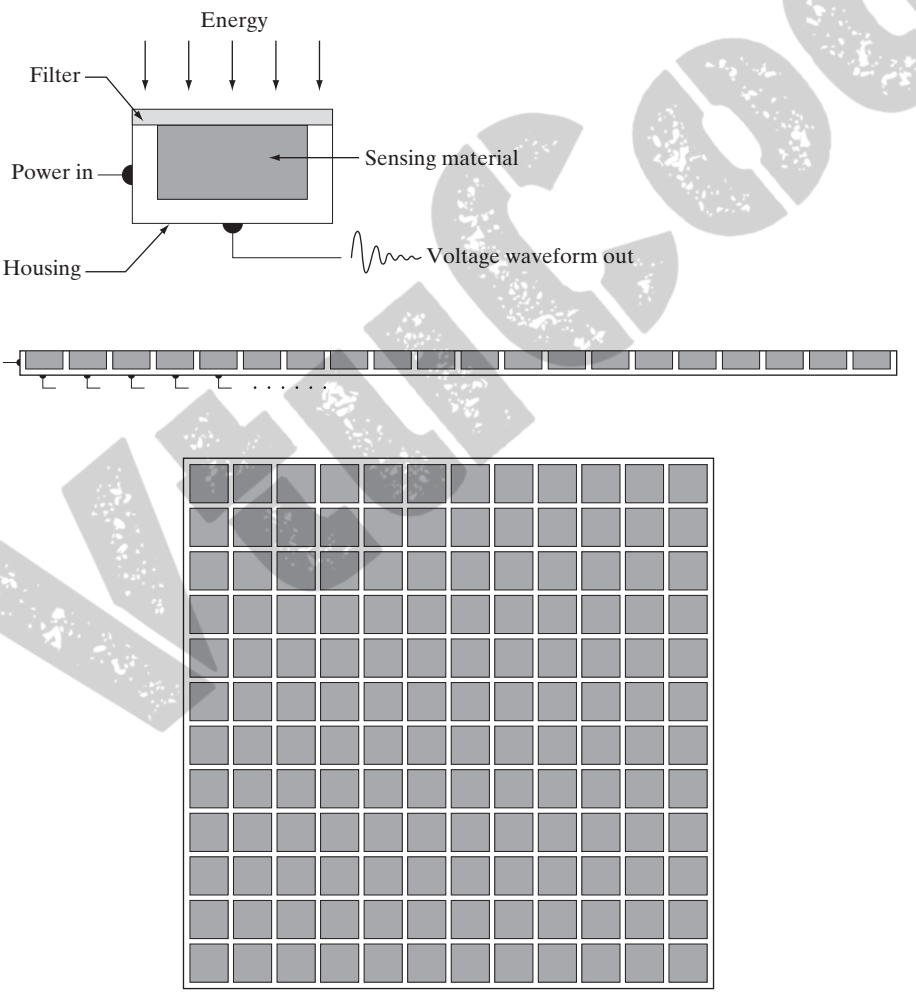

FIGURE 2.12
(a) Single imaging sensor.
(b) Line sensor.
(c) Array sensor.

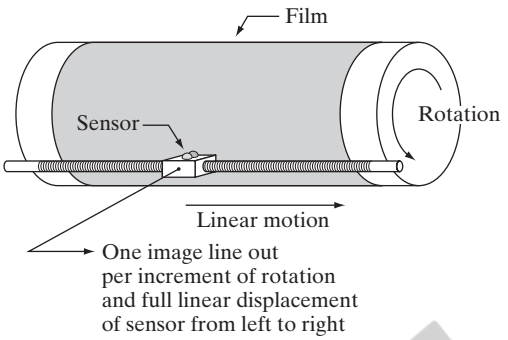

FIGURE 2.13 Combining a single sensor with motion to generate a 2-D image.

2.3.1 Image Acquisition Using a Single Sensor

Figure 2.12(a) shows the components of a single sensor. Perhaps the most familiar sensor of this type is the photodiode, which is constructed of silicon materials and whose output voltage waveform is proportional to light. The use of a filter in front of a sensor improves selectivity. For example, a green (pass) filter in front of a light sensor favors light in the green band of the color spectrum. As a consequence, the sensor output will be stronger for green light than for other components in the visible spectrum.

In order to generate a 2-D image using a single sensor, there has to be relative displacements in both the x- and y-directions between the sensor and the area to be imaged. Figure 2.13 shows an arrangement used in high-precision scanning, where a film negative is mounted onto a drum whose mechanical rotation provides displacement in one dimension. The single sensor is mounted on a lead screw that provides motion in the perpendicular direction. Because mechanical motion can be controlled with high precision, this method is an inexpensive (but slow) way to obtain high-resolution images. Other similar mechanical arrangements use a flat bed, with the sensor moving in two linear directions. These types of mechanical digitizers sometimes are referred to as *microdensitometers*.

Another example of imaging with a single sensor places a laser source coincident with the sensor. Moving mirrors are used to control the outgoing beam in a scanning pattern and to direct the reflected laser signal onto the sensor. This arrangement can be used also to acquire images using strip and array sensors, which are discussed in the following two sections.

2.3.2 Image Acquisition Using Sensor Strips

A geometry that is used much more frequently than single sensors consists of an in-line arrangement of sensors in the form of a sensor strip, as Fig. 2.12(b) shows. The strip provides imaging elements in one direction. Motion perpendicular to the strip provides imaging in the other direction, as shown in Fig. 2.14(a). This is the type of arrangement used in most flat bed scanners. Sensing devices with 4000 or more in-line sensors are possible. In-line sensors are used routinely in airborne imaging applications, in which the imaging system is mounted on an aircraft that

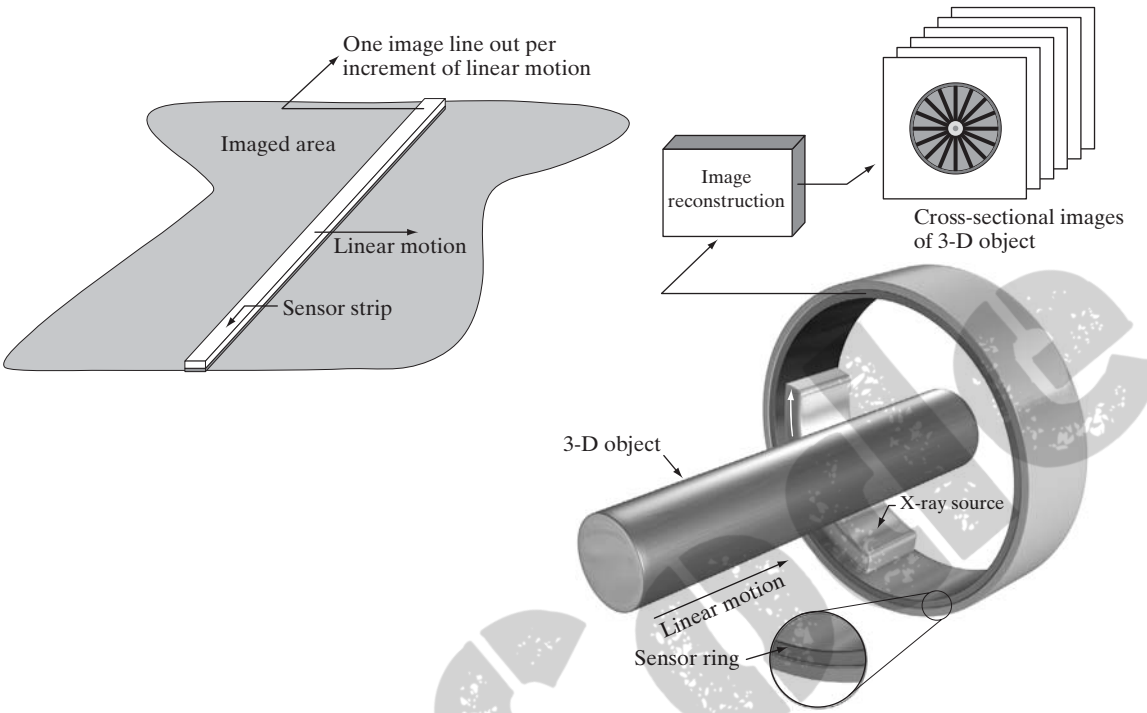

a b

FIGURE 2.14 (a) Image acquisition using a linear sensor strip. (b) Image acquisition using a circular sensor strip.

flies at a constant altitude and speed over the geographical area to be imaged. One-dimensional imaging sensor strips that respond to various bands of the electromagnetic spectrum are mounted perpendicular to the direction of flight. The imaging strip gives one line of an image at a time, and the motion of the strip completes the other dimension of a two-dimensional image. Lenses or other focusing schemes are used to project the area to be scanned onto the sensors.

Sensor strips mounted in a ring configuration are used in medical and industrial imaging to obtain cross-sectional ("slice") images of 3-D objects, as Fig. 2.14(b) shows. A rotating X-ray source provides illumination and the sensors opposite the source collect the X-ray energy that passes through the object (the sensors obviously have to be sensitive to X-ray energy). This is the basis for medical and industrial computerized axial tomography (CAT) imaging as indicated in Sections 1.2 and 1.3.2. It is important to note that the output of the sensors must be processed by reconstruction algorithms whose objective is to transform the sensed data into meaningful cross-sectional images (see Section 5.11). In other words, images are not obtained directly from the sensors by motion alone; they require extensive processing. A 3-D digital volume consisting of stacked images is generated as the object is moved in a direction

perpendicular to the sensor ring. Other modalities of imaging based on the CAT principle include magnetic resonance imaging (MRI) and positron emission tomography (PET). The illumination sources, sensors, and types of images are different, but conceptually they are very similar to the basic imaging approach shown in Fig. 2.14(b).

2.3.3 Image Acquisition Using Sensor Arrays

Figure 2.12(c) shows individual sensors arranged in the form of a 2-D array. Numerous electromagnetic and some ultrasonic sensing devices frequently are arranged in an array format. This is also the predominant arrangement found in digital cameras. A typical sensor for these cameras is a CCD array, which can be manufactured with a broad range of sensing properties and can be packaged in rugged arrays of 4000×4000 elements or more. CCD sensors are used widely in digital cameras and other light sensing instruments. The response of each sensor is proportional to the integral of the light energy projected onto the surface of the sensor, a property that is used in astronomical and other applications requiring low noise images. Noise reduction is achieved by letting the sensor integrate the input light signal over minutes or even hours. Because the sensor array in Fig. 2.12(c) is two-dimensional, its key advantage is that a complete image can be obtained by focusing the energy pattern onto the surface of the array. Motion obviously is not necessary, as is the case with the sensor arrangements discussed in the preceding two sections.

The principal manner in which array sensors are used is shown in Fig. 2.15. This figure shows the energy from an illumination source being reflected from a scene element (as mentioned at the beginning of this section, the energy also could be transmitted through the scene elements). The first function performed by the imaging system in Fig. 2.15(c) is to collect the incoming energy and focus it onto an image plane. If the illumination is light, the front end of the imaging system is an optical lens that projects the viewed scene onto the lens focal plane, as Fig. 2.15(d) shows. The sensor array, which is coincident with the focal plane, produces outputs proportional to the integral of the light received at each sensor. Digital and analog circuitry sweep these outputs and convert them to an analog signal, which is then digitized by another section of the imaging system. The output is a digital image, as shown diagrammatically in Fig. 2.15(e). Conversion of an image into digital form is the topic of Section 2.4.

In some cases, we image the source directly, as in obtaining images of the sun.

Image intensities can become negative during processing or as a result of interpretation. For example, in radar images objects moving toward a radar system often are interpreted as having negative velocities while objects moving away are interpreted as having positive velocities. Thus, a velocity image might be coded as having both positive and negative values. When storing and displaying images, we normally scale the intensities so that the smallest negative value becomes 0 (see Section 2.6.3 regarding intensity scaling).

2.3.4 A Simple Image Formation Model

As introduced in Section 1.1, we denote images by two-dimensional functions of the form $f(x, y)$. The value or amplitude of f at spatial coordinates (x, y) is a positive scalar quantity whose physical meaning is determined by the source of the image. When an image is generated from a physical process, its intensity values are proportional to energy radiated by a physical source (e.g., electromagnetic waves). As a consequence, $f(x, y)$ must be nonzero

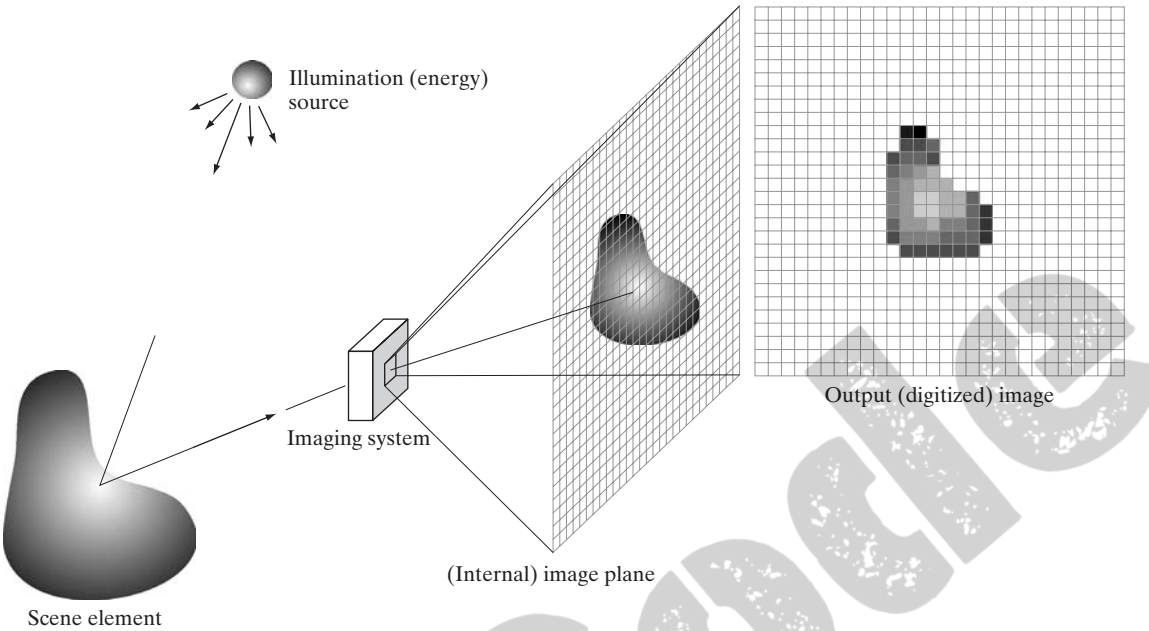

a
b c d e

FIGURE 2.15 An example of the digital image acquisition process. (a) Energy ("illumination") source. (b) An element of a scene. (c) Imaging system. (d) Projection of the scene onto the image plane. (e) Digitized image.

and finite; that is,

$$0 < f(x, y) < \infty \tag{2.3-1}$$

The function $f(x, y)$ may be characterized by two components: (1) the amount of source illumination incident on the scene being viewed, and (2) the amount of illumination reflected by the objects in the scene. Appropriately, these are called the *illumination* and *reflectance* components and are denoted by $i(x, y)$ and $r(x, y)$, respectively. The two functions combine as a product to form $f(x, y)$:

$$f(x, y) = i(x, y)r(x, y) \tag{2.3-2}$$

where

$$0 < i(x, y) < \infty \tag{2.3-3}$$

and

$$0 < r(x, y) < 1 \tag{2.3-4}$$

Equation (2.3-4) indicates that reflectance is bounded by 0 (total absorption) and 1 (total reflectance). The nature of $i(x, y)$ is determined by the illumination source, and $r(x, y)$ is determined by the characteristics of the imaged objects. It is noted that these expressions also are applicable to images formed via transmission of the illumination through a medium, such as a chest X-ray.

In this case, we would deal with a *transmissivity* instead of a *reflectivity* function, but the limits would be the same as in Eq. (2.3-4), and the image function formed would be modeled as the product in Eq. (2.3-2).

EXAMPLE 2.1: Some typical values of illumination and reflectance.

■ The values given in Eqs. (2.3-3) and (2.3-4) are theoretical bounds. The following *average* numerical figures illustrate some typical ranges of $i(x, y)$ for visible light. On a clear day, the sun may produce in excess of 90,000 lm/m^2 of illumination on the surface of the Earth. This figure decreases to less than 10,000 lm/m^2 on a cloudy day. On a clear evening, a full moon yields about 0.1 lm/m^2 of illumination. The typical illumination level in a commercial office is about 1000 lm/m^2. Similarly, the following are typical values of $r(x, y)$: 0.01 for black velvet, 0.65 for stainless steel, 0.80 for flat-white wall paint, 0.90 for silver-plated metal, and 0.93 for snow. ■

Let the intensity (gray level) of a monochrome image at any coordinates (x_0, y_0) be denoted by

$$\ell = f(x_0, y_0) \tag{2.3-5}$$

From Eqs. (2.3-2) through (2.3-4), it is evident that ℓ lies in the range

$$L_{\min} \leq \ell \leq L_{\max} \tag{2.3-6}$$

In theory, the only requirement on $L_{\min}$ is that it be positive, and on $L_{\max}$ that it be finite. In practice, $L_{\min} = i_{\min} r_{\min}$ and $L_{\max} = i_{\max} r_{\max}$. Using the preceding average office illumination and range of reflectance values as guidelines, we may expect $L_{\min} \approx 10$ and $L_{\max} \approx 1000$ to be typical limits for indoor values in the absence of additional illumination.

The interval $[L_{\min}, L_{\max}]$ is called the *gray* (or *intensity*) *scale*. Common practice is to shift this interval numerically to the interval $[0, L - 1]$, where $\ell = 0$ is considered black and $\ell = L - 1$ is considered white on the gray scale. All intermediate values are shades of gray varying from black to white.

2.4 Image Sampling and Quantization

The discussion of sampling in this section is of an intuitive nature. We consider this topic in depth in Chapter 4.

From the discussion in the preceding section, we see that there are numerous ways to acquire images, but our objective in all is the same: to generate digital images from sensed data. The output of most sensors is a continuous voltage waveform whose amplitude and spatial behavior are related to the physical phenomenon being sensed. To create a digital image, we need to convert the continuous sensed data into digital form. This involves two processes: *sampling* and *quantization*.

2.4.1 Basic Concepts in Sampling and Quantization

The basic idea behind sampling and quantization is illustrated in Fig. 2.16. Figure 2.16(a) shows a continuous image f that we want to convert to digital form. An image may be continuous with respect to the x- and y-coordinates, and also in amplitude. To convert it to digital form, we have to sample the

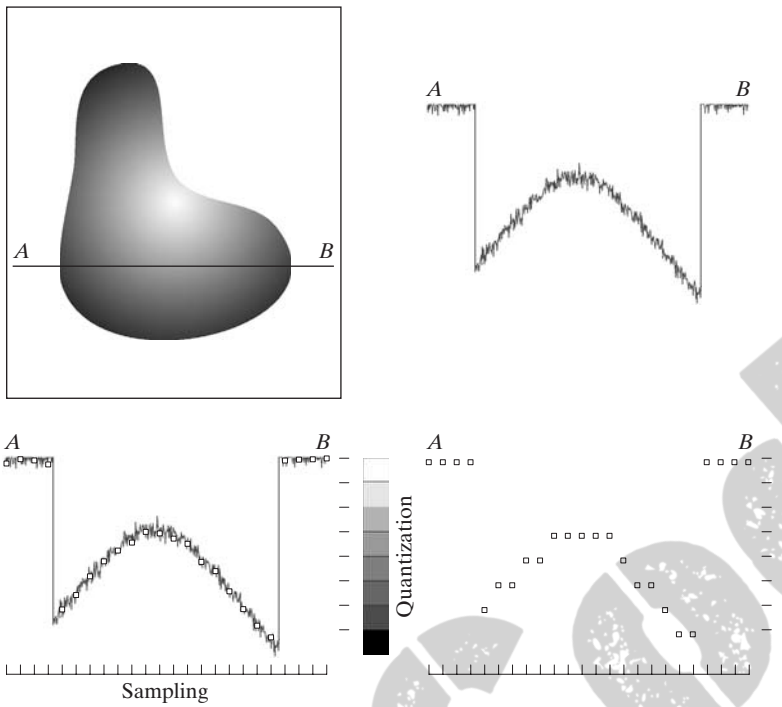

a b
c d

FIGURE 2.16 Generating a digital image. (a) Continuous image. (b) A scan line from *A* to *B* in the continuous image, used to illustrate the concepts of sampling and quantization. (c) Sampling and quantization. (d) Digital scan line.

function in both coordinates and in amplitude. Digitizing the coordinate values is called *sampling*. Digitizing the amplitude values is called *quantization*.

The one-dimensional function in Fig. 2.16(b) is a plot of amplitude (intensity level) values of the continuous image along the line segment *AB* in Fig. 2.16(a). The random variations are due to image noise. To sample this function, we take equally spaced samples along line *AB*, as shown in Fig. 2.16(c). The spatial location of each sample is indicated by a vertical tick mark in the bottom part of the figure. The samples are shown as small white squares superimposed on the function. The set of these discrete locations gives the sampled function. However, the values of the samples still span (vertically) a continuous range of intensity values. In order to form a digital function, the intensity values also must be converted (*quantized*) into discrete quantities. The right side of Fig. 2.16(c) shows the intensity scale divided into eight discrete intervals, ranging from black to white. The vertical tick marks indicate the specific value assigned to each of the eight intensity intervals. The continuous intensity levels are quantized by assigning one of the eight values to each sample. The assignment is made depending on the vertical proximity of a sample to a vertical tick mark. The digital samples resulting from both sampling and quantization are shown in Fig. 2.16(d). Starting at the top of the image and carrying out this procedure line by line produces a two-dimensional digital image. It is implied in Fig. 2.16 that, in addition to the number of discrete levels used, the accuracy achieved in quantization is highly dependent on the noise content of the sampled signal.

Sampling in the manner just described assumes that we have a continuous image in both coordinate directions as well as in amplitude. In practice, the

method of sampling is determined by the sensor arrangement used to generate the image. When an image is generated by a single sensing element combined with mechanical motion, as in Fig. 2.13, the output of the sensor is quantized in the manner described above. However, spatial sampling is accomplished by selecting the number of individual mechanical increments at which we activate the sensor to collect data. Mechanical motion can be made very exact so, in principle, there is almost no limit as to how fine we can sample an image using this approach. In practice, limits on sampling accuracy are determined by other factors, such as the quality of the optical components of the system.

When a sensing strip is used for image acquisition, the number of sensors in the strip establishes the sampling limitations in one image direction. Mechanical motion in the other direction can be controlled more accurately, but it makes little sense to try to achieve sampling density in one direction that exceeds the sampling limits established by the number of sensors in the other. Quantization of the sensor outputs completes the process of generating a digital image.

When a sensing array is used for image acquisition, there is no motion and the number of sensors in the array establishes the limits of sampling in both directions. Quantization of the sensor outputs is as before. Figure 2.17 illustrates this concept. Figure 2.17(a) shows a continuous image projected onto the plane of an array sensor. Figure 2.17(b) shows the image after sampling and quantization. Clearly, the quality of a digital image is determined to a large degree by the number of samples and discrete intensity levels used in sampling and quantization. However, as we show in Section 2.4.3, image content is also an important consideration in choosing these parameters.

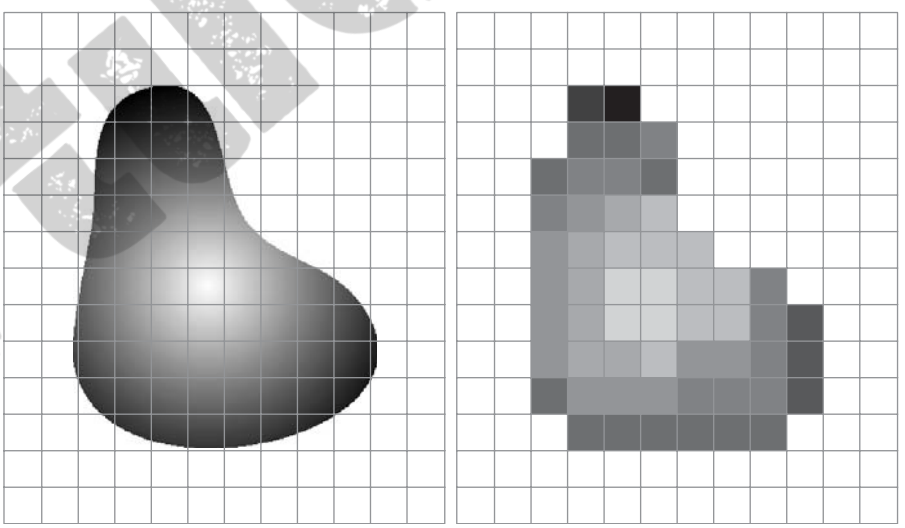

a b

FIGURE 2.17 (a) Continuous image projected onto a sensor array. (b) Result of image sampling and quantization.

2.4.2 Representing Digital Images

Let $f(s, t)$ represent a continuous image function of two continuous variables, s and t. We convert this function into a *digital image* by sampling and quantization, as explained in the previous section. Suppose that we sample the continuous image into a 2-D array, $f(x, y)$, containing M rows and N columns, where (x, y) are discrete coordinates. For notational clarity and convenience, we use integer values for these discrete coordinates: $x = 0, 1, 2, \ldots, M - 1$ and $y = 0, 1, 2, \ldots, N - 1$. Thus, for example, the value of the digital image at the origin is $f(0, 0)$, and the next coordinate value along the first row is $f(0, 1)$. Here, the notation $(0, 1)$ is used to signify the second sample along the first row. It *does not* mean that these are the values of the physical coordinates when the image was sampled. In general, the value of the image at any coordinates (x, y) is denoted $f(x, y)$, where x and y are integers. The section of the real plane spanned by the coordinates of an image is called the *spatial domain*, with x and y being referred to as *spatial variables* or *spatial coordinates*.

As Fig. 2.18 shows, there are three basic ways to represent $f(x, y)$. Figure 2.18(a) is a plot of the function, with two axes determining spatial location

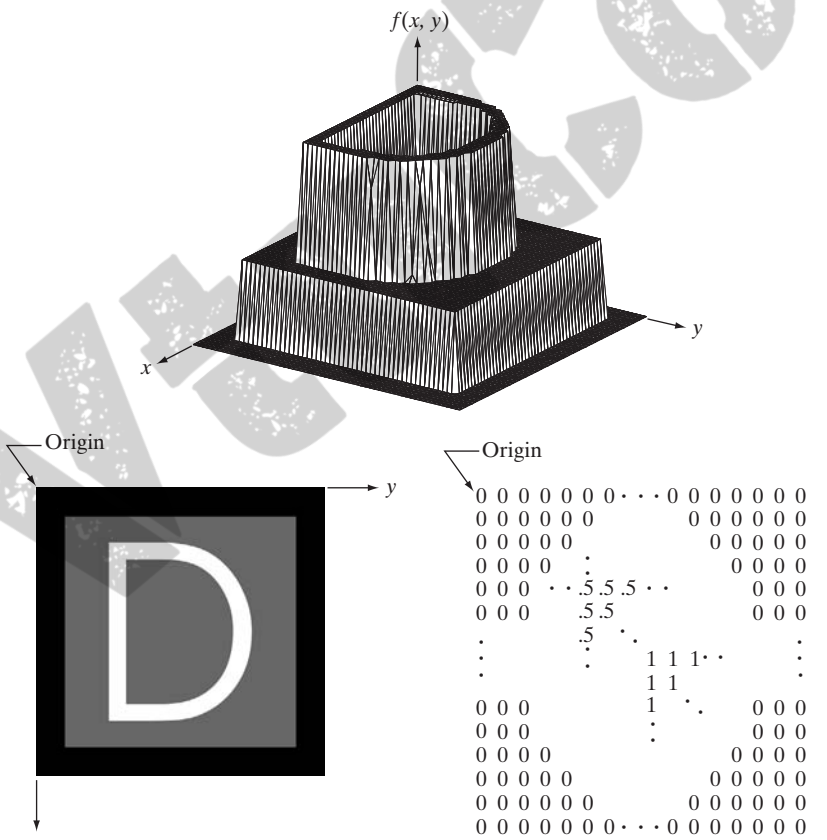

a
b c

FIGURE 2.18
(a) Image plotted as a surface.
(b) Image displayed as a visual intensity array.
(c) Image shown as a 2-D numerical array (0, .5, and 1 represent black, gray, and white, respectively).

and the third axis being the values of f (intensities) as a function of the two spatial variables x and y. Although we can infer the structure of the image in this example by looking at the plot, complex images generally are too detailed and difficult to interpret from such plots. This representation is useful when working with gray-scale sets whose elements are expressed as triplets of the form (x, y, z), where x and y are spatial coordinates and z is the value of f at coordinates (x, y). We work with this representation in Section 2.6.4.

The representation in Fig. 2.18(b) is much more common. It shows $f(x, y)$ as it would appear on a monitor or photograph. Here, the intensity of each point is proportional to the value of f at that point. In this figure, there are only three equally spaced intensity values. If the intensity is normalized to the interval [0, 1], then each point in the image has the value 0, 0.5, or 1. A monitor or printer simply converts these three values to black, gray, or white, respectively, as Fig. 2.18(b) shows. The third representation is simply to display the numerical values of $f(x, y)$ as an array (matrix). In this example, f is of size 600×600 elements, or 360,000 numbers. Clearly, printing the complete array would be cumbersome and convey little information. When developing algorithms, however, this representation is quite useful when only parts of the image are printed and analyzed as numerical values. Figure 2.18(c) conveys this concept graphically.

We conclude from the previous paragraph that the representations in Figs. 2.18(b) and (c) are the most useful. Image displays allow us to view results at a glance. Numerical arrays are used for processing and algorithm development. In equation form, we write the representation of an $M \times N$ numerical array as

$$f(x, y) = \begin{bmatrix} f(0, 0) & f(0, 1) & \cdots & f(0, N-1) \\ f(1, 0) & f(1, 1) & \cdots & f(1, N-1) \\ \vdots & \vdots & & \vdots \\ f(M-1, 0) & f(M-1, 1) & \cdots & f(M-1, N-1) \end{bmatrix} \quad (2.4\text{-}1)$$

Both sides of this equation are equivalent ways of expressing a digital image quantitatively. The right side is a matrix of real numbers. Each element of this matrix is called an *image element, picture element, pixel*, or *pel*. The terms *image* and *pixel* are used throughout the book to denote a digital image and its elements.

In some discussions it is advantageous to use a more traditional matrix notation to denote a digital image and its elements:

$$\mathbf{A} = \begin{bmatrix} a_{0,0} & a_{0,1} & \cdots & a_{0,N-1} \\ a_{1,0} & a_{1,1} & \cdots & a_{1,N-1} \\ \vdots & \vdots & & \vdots \\ a_{M-1,0} & a_{M-1,1} & \cdots & a_{M-1,N-1} \end{bmatrix} \quad (2.4\text{-}2)$$

Clearly, $a_{ij} = f(x = i, y = j) = f(i, j)$, so Eqs. (2.4-1) and (2.4-2) are identical matrices. We can even represent an image as a vector, $\mathbf{v}$. For example, a column vector of size $MN \times 1$ is formed by letting the first M elements of $\mathbf{v}$ be the first column of $\mathbf{A}$, the next M elements be the second column, and so on. Alternatively, we can use the rows instead of the columns of $\mathbf{A}$ to form such a vector. Either representation is valid, as long as we are consistent.

Returning briefly to Fig. 2.18, note that the origin of a digital image is at the top left, with the positive x-axis extending downward and the positive y-axis extending to the right. This is a conventional representation based on the fact that many image displays (e.g., TV monitors) sweep an image starting at the top left and moving to the right one row at a time. More important is the fact that the first element of a matrix is by convention at the top left of the array, so choosing the origin of $f(x, y)$ at that point makes sense mathematically. Keep in mind that this representation is the standard right-handed Cartesian coordinate system with which you are familiar.[†] We simply show the axes pointing downward and to the right, instead of to the right and up.

Expressing sampling and quantization in more formal mathematical terms can be useful at times. Let Z and R denote the set of integers and the set of real numbers, respectively. The sampling process may be viewed as partitioning the xy-plane into a grid, with the coordinates of the center of each cell in the grid being a pair of elements from the Cartesian product Z^2, which is the set of all ordered pairs of elements (z_i, z_j), with z_i and z_j being integers from Z. Hence, $f(x, y)$ is a digital image if (x, y) are integers from Z^2 and f is a function that assigns an intensity value (that is, a real number from the set of real numbers, R) to each distinct pair of coordinates (x, y). This functional assignment is the quantization process described earlier. If the intensity levels also are integers (as usually is the case in this and subsequent chapters), Z replaces R, and a digital image then becomes a 2-D function whose coordinates and amplitude values are integers.

This digitization process requires that decisions be made regarding the values for M, N, and for the number, L, of discrete intensity levels. There are no restrictions placed on M and N, other than they have to be positive integers. However, due to storage and quantizing hardware considerations, the number of intensity levels typically is an integer power of 2:

$$L = 2^k \tag{2.4-3}$$

We assume that the discrete levels are equally spaced and that they are integers in the interval $[0, L - 1]$. Sometimes, the range of values spanned by the gray scale is referred to informally as the dynamic range. This is a term used in different ways in different fields. Here, we define the *dynamic range* of an imaging system to be the ratio of the maximum measurable intensity to the minimum

Often, it is useful for computation or for algorithm development purposes to scale the L intensity values to the range $[0, 1]$, in which case they cease to be integers. However, in most cases these values are scaled back to the integer range $[0, L - 1]$ for image storage and display.

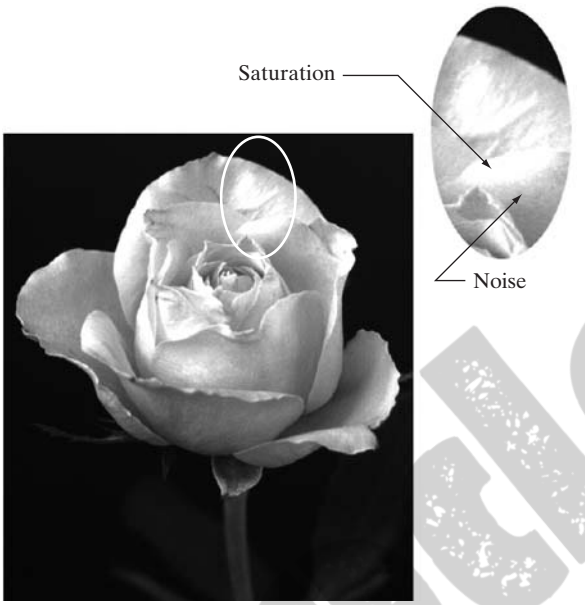

FIGURE 2.19 An image exhibiting saturation and noise. Saturation is the highest value beyond which all intensity levels are clipped (note how the entire saturated area has a high, *constant* intensity level). Noise in this case appears as a grainy texture pattern. Noise, especially in the darker regions of an image (e.g., the stem of the rose) masks the lowest detectable true intensity level.

detectable intensity level in the system. As a rule, the upper limit is determined by *saturation* and the lower limit by *noise* (see Fig. 2.19). Basically, dynamic range establishes the lowest and highest intensity levels that a system can represent and, consequently, that an image can have. Closely associated with this concept is image *contrast*, which we define as the difference in intensity between the highest and lowest intensity levels in an image. When an appreciable number of pixels in an image have a high dynamic range, we can expect the image to have high contrast. Conversely, an image with low dynamic range typically has a dull, washed-out gray look. We discuss these concepts in more detail in Chapter 3.

The number, b, of bits required to store a digitized image is

$$b = M \times N \times k \tag{2.4-4}$$

When $M = N$, this equation becomes

$$b = N^2 k \tag{2.4-5}$$

Table 2.1 shows the number of bits required to store square images with various values of N and k. The number of intensity levels corresponding to each value of k is shown in parentheses. When an image can have 2^k intensity levels, it is common practice to refer to the image as a "k-bit image." For example, an image with 256 possible discrete intensity values is called an 8-bit image. Note that storage requirements for 8-bit images of size 1024×1024 and higher are not insignificant.

TABLE 2.1
Number of storage bits for various values of N and k. L is the number of intensity levels.

N/k	1 ($L = 2$)	2 ($L = 4$)	3 ($L = 8$)	4 ($L = 16$)	5 ($L = 32$)	6 ($L = 64$)	7 ($L = 128$)	8 ($L = 256$)
32	1,024	2,048	3,072	4,096	5,120	6,144	7,168	8,192
64	4,096	8,192	12,288	16,384	20,480	24,576	28,672	32,768
128	16,384	32,768	49,152	65,536	81,920	98,304	114,688	131,072
256	65,536	131,072	196,608	262,144	327,680	393,216	458,752	524,288
512	262,144	524,288	786,432	1,048,576	1,310,720	1,572,864	1,835,008	2,097,152
1024	1,048,576	2,097,152	3,145,728	4,194,304	5,242,880	6,291,456	7,340,032	8,388,608
2048	4,194,304	8,388,608	12,582,912	16,777,216	20,971,520	25,165,824	29,369,128	33,554,432
4096	16,777,216	33,554,432	50,331,648	67,108,864	83,886,080	100,663,296	117,440,512	134,217,728
8192	67,108,864	134,217,728	201,326,592	268,435,456	335,544,320	402,653,184	469,762,048	536,870,912

2.4.3 Spatial and Intensity Resolution

Intuitively, spatial resolution is a measure of the smallest discernible detail in an image. Quantitatively, *spatial resolution* can be stated in a number of ways, with *line pairs per unit distance*, and *dots* (*pixels*) *per unit distance* being among the most common measures. Suppose that we construct a chart with alternating black and white vertical lines, each of width W units (W can be less than 1). The width of a *line pair* is thus $2W$, and there are $1/2W$ line pairs per unit distance. For example, if the width of a line is 0.1 mm, there are 5 line pairs per unit distance (mm). A widely used definition of image resolution is the largest number of *discernible* line pairs per unit distance (e.g., 100 line pairs per mm). Dots per unit distance is a measure of image resolution used commonly in the printing and publishing industry. In the U.S., this measure usually is expressed as *dots per inch* (dpi). To give you an idea of quality, newspapers are printed with a resolution of 75 dpi, magazines at 133 dpi, glossy brochures at 175 dpi, and the book page at which you are presently looking is printed at 2400 dpi.

The key point in the preceding paragraph is that, to be meaningful, measures of spatial resolution must be stated with respect to spatial units. Image size by itself does not tell the complete story. To say that an image has, say, a resolution 1024×1024 pixels is not a meaningful statement without stating the spatial dimensions encompassed by the image. Size by itself is helpful only in making comparisons between imaging capabilities. For example, a digital camera with a 20-megapixel CCD imaging chip can be expected to have a higher capability to resolve detail than an 8-megapixel camera, assuming that both cameras are equipped with comparable lenses and the comparison images are taken at the same distance.

Intensity resolution similarly refers to the smallest discernible change in intensity level. We have considerable discretion regarding the number of samples used to generate a digital image, but this is not true regarding the number

of intensity levels. Based on hardware considerations, the number of intensity levels usually is an integer power of two, as mentioned in the previous section. The most common number is 8 bits, with 16 bits being used in some applications in which enhancement of specific intensity ranges is necessary. Intensity quantization using 32 bits is rare. Sometimes one finds systems that can digitize the intensity levels of an image using 10 or 12 bits, but these are the exception, rather than the rule. Unlike spatial resolution, which must be based on a per unit of distance basis to be meaningful, it is common practice to refer to the number of bits used to quantize intensity as the *intensity resolution*. For example, it is common to say that an image whose intensity is quantized into 256 levels has 8 bits of intensity resolution. Because true discernible changes in intensity are influenced not only by noise and saturation values but also by the capabilities of human perception (see Section 2.1), saying than an image has 8 bits of intensity resolution is nothing more than a statement regarding the ability of an 8-bit system to quantize intensity in fixed increments of 1/256 units of intensity amplitude.

The following two examples illustrate individually the comparative effects of image size and intensity resolution on discernable detail. Later in this section, we discuss how these two parameters interact in determining perceived image quality.

EXAMPLE 2.2: Illustration of the effects of reducing image spatial resolution.

■ Figure 2.20 shows the effects of reducing spatial resolution in an image. The images in Figs. 2.20(a) through (d) are shown in 1250, 300, 150, and 72 dpi, respectively. Naturally, the lower resolution images are smaller than the original. For example, the original image is of size 3692×2812 pixels, but the 72 dpi image is an array of size 213×162. In order to facilitate comparisons, all the smaller images were zoomed back to the original size (the method used for zooming is discussed in Section 2.4.4). This is somewhat equivalent to "getting closer" to the smaller images so that we can make comparable statements about visible details.

There are some small visual differences between Figs. 2.20(a) and (b), the most notable being a slight distortion in the large black needle. For the most part, however, Fig. 2.20(b) is quite acceptable. In fact, 300 dpi is the typical minimum image spatial resolution used for book publishing, so one would not expect to see much difference here. Figure 2.20(c) begins to show visible degradation (see, for example, the round edges of the chronometer and the small needle pointing to 60 on the right side). Figure 2.20(d) shows degradation that is visible in most features of the image. As we discuss in Section 4.5.4, when printing at such low resolutions, the printing and publishing industry uses a number of "tricks" (such as locally varying the pixel size) to produce much better results than those in Fig. 2.20(d). Also, as we show in Section 2.4.4, it is possible to improve on the results of Fig. 2.20 by the choice of interpolation method used. ■

a b
c d

FIGURE 2.20 Typical effects of reducing spatial resolution. Images shown at: (a) 1250 dpi, (b) 300 dpi, (c) 150 dpi, and (d) 72 dpi. The thin black borders were added for clarity. They are not part of the data.

EXAMPLE 2.3: Typical effects of varying the number of intensity levels in a digital image.

■ In this example, we keep the number of samples constant and reduce the number of intensity levels from 256 to 2, in integer powers of 2. Figure 2.21(a) is a 452 × 374 CT projection image, displayed with $k = 8$ (256 intensity levels). Images such as this are obtained by fixing the X-ray source in one position, thus producing a 2-D image in any desired direction. Projection images are used as guides to set up the parameters for a CT scanner, including tilt, number of slices, and range.

Figures 2.21(b) through (h) were obtained by reducing the number of bits from $k = 7$ to $k = 1$ while keeping the image size constant at 452 × 374 pixels. The 256-, 128-, and 64-level images are visually identical for all practical purposes. The 32-level image in Fig. 2.21(d), however, has an imperceptible set of

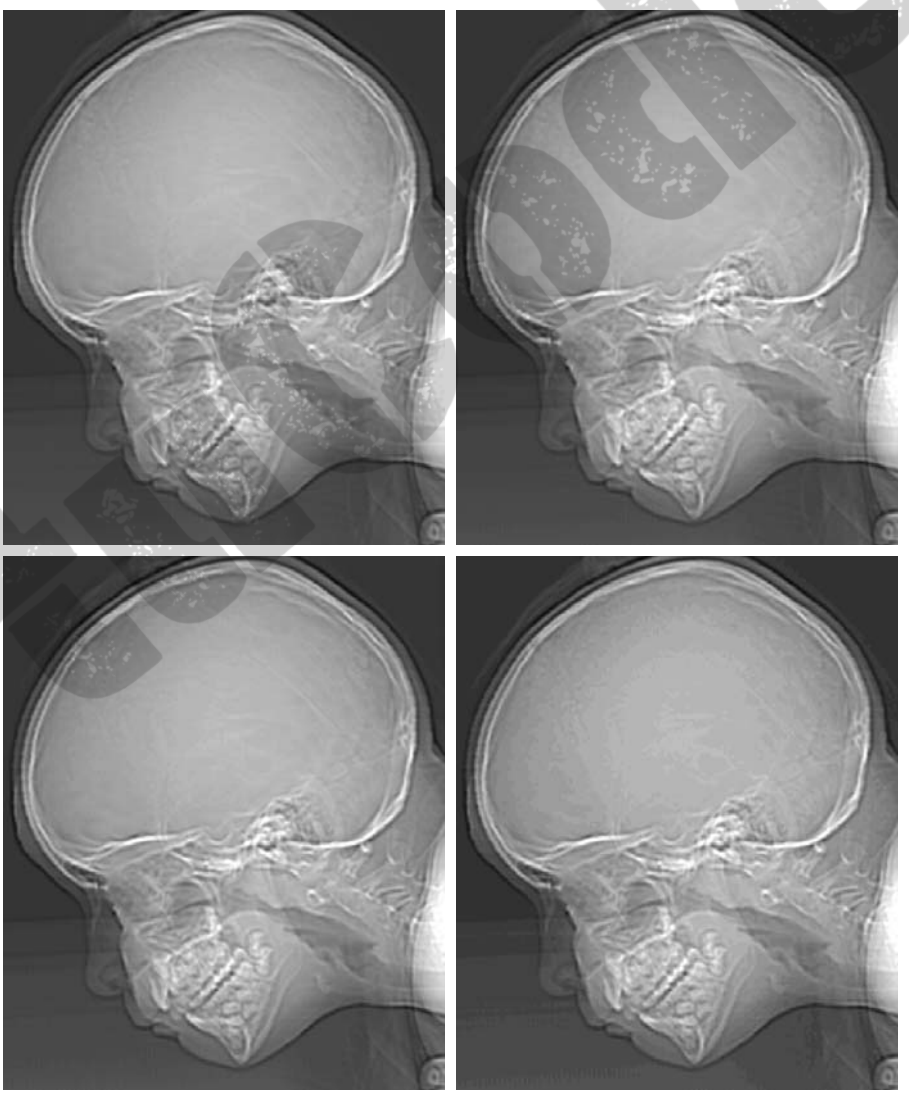

a b
c d

FIGURE 2.21 (a) 452 × 374, 256-level image. (b)–(d) Image displayed in 128, 64, and 32 intensity levels, while keeping the image size constant.

very fine ridge-like structures in areas of constant or nearly constant intensity (particularly in the skull). This effect, caused by the use of an insufficient number of intensity levels in smooth areas of a digital image, is called *false contouring*, so called because the ridges resemble topographic contours in a map. False contouring generally is quite visible in images displayed using 16 or less uniformly spaced intensity levels, as the images in Figs. 2.21(e) through (h) show.

As a very rough rule of thumb, and assuming integer powers of 2 for convenience, images of size 256 × 256 pixels with 64 intensity levels and printed on a size format on the order of 5 × 5 cm are about the lowest spatial and intensity resolution images that can be expected to be reasonably free of objectionable sampling checkerboards and false contouring. ■

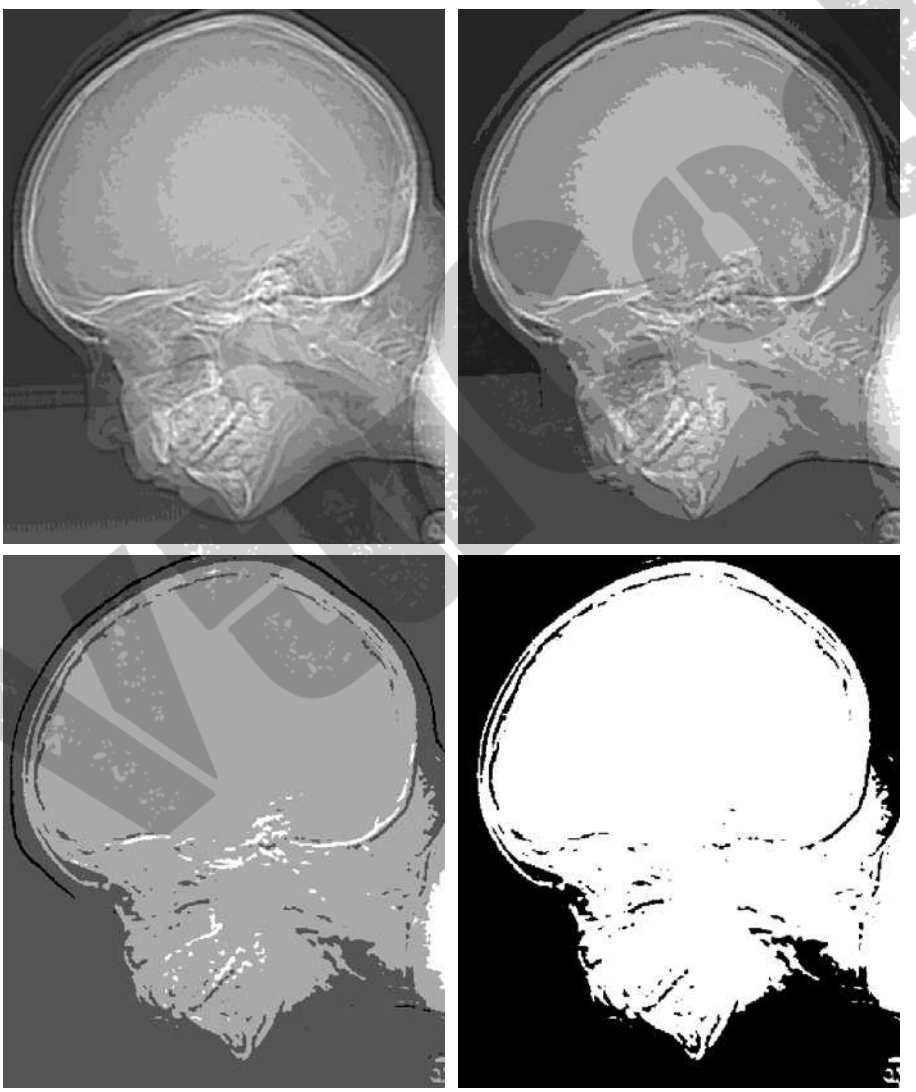

e f
g h

FIGURE 2.21 (*Continued*) (e)–(h) Image displayed in 16, 8, 4, and 2 intensity levels. (Original courtesy of Dr. David R. Pickens, Department of Radiology & Radiological Sciences, Vanderbilt University Medical Center.)

a b c

FIGURE 2.22 (a) Image with a low level of detail. (b) Image with a medium level of detail. (c) Image with a relatively large amount of detail. (Image (b) courtesy of the Massachusetts Institute of Technology.)

The results in Examples 2.2 and 2.3 illustrate the effects produced on image quality by varying N and k independently. However, these results only partially answer the question of how varying N and k affects images because we have not considered yet any relationships that might exist between these two parameters. An early study by Huang [1965] attempted to quantify experimentally the effects on image quality produced by varying N and k simultaneously. The experiment consisted of a set of subjective tests. Images similar to those shown in Fig. 2.22 were used. The woman's face is representative of an image with relatively little detail; the picture of the cameraman contains an intermediate amount of detail; and the crowd picture contains, by comparison, a large amount of detail.

Sets of these three types of images were generated by varying N and k, and observers were then asked to rank them according to their subjective quality. Results were summarized in the form of so-called *isopreference curves* in the Nk-plane. (Figure 2.23 shows average isopreference curves representative of curves corresponding to the images in Fig. 2.22.) Each point in the Nk-plane represents an image having values of N and k equal to the coordinates of that point. Points lying on an isopreference curve correspond to images of equal subjective quality. It was found in the course of the experiments that the isopreference curves tended to shift right and upward, but their shapes in each of the three image categories were similar to those in Fig. 2.23. This is not unexpected, because a shift up and right in the curves simply means larger values for N and k, which implies better picture quality.

The key point of interest in the context of the present discussion is that isopreference curves tend to become more vertical as the detail in the image increases. This result suggests that for images with a large amount of detail only a few intensity levels may be needed. For example, the isopreference curve in Fig. 2.23 corresponding to the crowd is nearly vertical. This indicates that, for a fixed value of N, the perceived quality for this type of image is

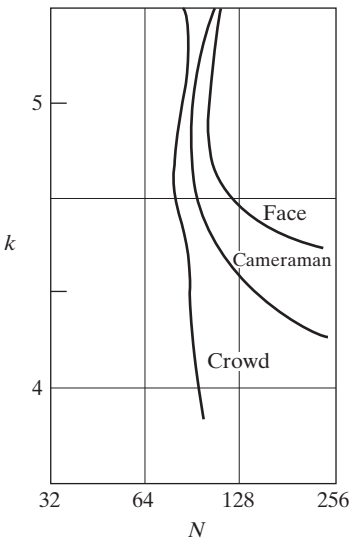

FIGURE 2.23 Typical isopreference curves for the three types of images in Fig. 2.22.

nearly independent of the number of intensity levels used (for the range of intensity levels shown in Fig. 2.23). It is of interest also to note that perceived quality in the other two image categories remained the same in some intervals in which the number of samples was increased, but the number of intensity levels actually decreased. The most likely reason for this result is that a decrease in k tends to increase the apparent contrast, a visual effect that humans often perceive as improved quality in an image.

2.4.4 Image Interpolation

Interpolation is a basic tool used extensively in tasks such as zooming, shrinking, rotating, and geometric corrections. Our principal objective in this section is to introduce interpolation and apply it to image resizing (shrinking and zooming), which are basically image *resampling* methods. Uses of interpolation in applications such as rotation and geometric corrections are discussed in Section 2.6.5. We also return to this topic in Chapter 4, where we discuss image resampling in more detail.

Fundamentally, *interpolation* is the process of using known data to estimate values at unknown locations. We begin the discussion of this topic with a simple example. Suppose that an image of size 500×500 pixels has to be enlarged 1.5 times to 750×750 pixels. A simple way to visualize zooming is to create an imaginary 750×750 grid with the same pixel spacing as the original, and then shrink it so that it fits exactly over the original image. Obviously, the pixel spacing in the shrunken 750×750 grid will be less than the pixel spacing in the original image. To perform intensity-level assignment for any point in the overlay, we look for its closest pixel in the original image and assign the intensity of that pixel to the new pixel in the 750×750 grid. When we are finished assigning intensities to all the points in the overlay grid, we expand it to the original specified size to obtain the zoomed image.

The method just discussed is called *nearest neighbor interpolation* because it assigns to each new location the intensity of its nearest neighbor in the original image (pixel neighborhoods are discussed formally in Section 2.5). This approach is simple but, as we show later in this section, it has the tendency to produce undesirable artifacts, such as severe distortion of straight edges. For this reason, it is used infrequently in practice. A more suitable approach is *bilinear interpolation*, in which we use the four nearest neighbors to estimate the intensity at a given location. Let (x, y) denote the coordinates of the location to which we want to assign an intensity value (think of it as a point of the grid described previously), and let $v(x, y)$ denote that intensity value. For bilinear interpolation, the assigned value is obtained using the equation

$$v(x, y) = ax + by + cxy + d \tag{2.4-6}$$

Contrary to what the name suggests, note that bilinear interpolation is *not* linear because of the xy term.

where the four coefficients are determined from the four equations in four unknowns that can be written using the four nearest neighbors of point (x, y). As you will see shortly, bilinear interpolation gives much better results than nearest neighbor interpolation, with a modest increase in computational burden.

The next level of complexity is *bicubic interpolation*, which involves the sixteen nearest neighbors of a point. The intensity value assigned to point (x, y) is obtained using the equation

$$v(x, y) = \sum_{i=0}^{3}\sum_{j=0}^{3} a_{ij}x^i y^j \tag{2.4-7}$$

where the sixteen coefficients are determined from the sixteen equations in sixteen unknowns that can be written using the sixteen nearest neighbors of point (x, y). Observe that Eq. (2.4-7) reduces in form to Eq. (2.4-6) if the limits of both summations in the former equation are 0 to 1. Generally, bicubic interpolation does a better job of preserving fine detail than its bilinear counterpart. Bicubic interpolation is the standard used in commercial image editing programs, such as Adobe Photoshop and Corel Photopaint.

EXAMPLE 2.4: Comparison of interpolation approaches for image shrinking and zooming.

■ Figure 2.24(a) is the same image as Fig. 2.20(d), which was obtained by reducing the resolution of the 1250 dpi image in Fig. 2.20(a) to 72 dpi (the size shrank from the original size of 3692 × 2812 to 213 × 162 pixels) and then zooming the reduced image back to its original size. To generate Fig. 2.20(d) we used nearest neighbor interpolation both to shrink and zoom the image. As we commented before, the result in Fig. 2.24(a) is rather poor. Figures 2.24(b) and (c) are the results of repeating the same procedure but using, respectively, bilinear and bicubic interpolation for both shrinking and zooming. The result obtained by using bilinear interpolation is a significant improvement over nearest neighbor interpolation. The bicubic result is slightly sharper than the bilinear image. Figure 2.24(d) is the same as Fig. 2.20(c), which was obtained using nearest neighbor interpolation for both shrinking and zooming. We commented in discussing that figure that reducing the resolution to 150 dpi began showing degradation in the image. Figures 2.24(e) and (f) show the results of using

a b c
d e f

FIGURE 2.24 (a) Image reduced to 72 dpi and zoomed back to its original size (3692 × 2812 pixels) using nearest neighbor interpolation. This figure is the same as Fig. 2.20(d). (b) Image shrunk and zoomed using bilinear interpolation. (c) Same as (b) but using bicubic interpolation. (d)–(f) Same sequence, but shrinking down to 150 dpi instead of 72 dpi [Fig. 2.24(d) is the same as Fig. 2.20(c)]. Compare Figs. 2.24(e) and (f), especially the latter, with the original image in Fig. 2.20(a).

bilinear and bicubic interpolation, respectively, to shrink and zoom the image. In spite of a reduction in resolution from 1250 to 150, these last two images compare reasonably favorably with the original, showing once again the power of these two interpolation methods. As before, bicubic interpolation yielded slightly sharper results. ■

It is possible to use more neighbors in interpolation, and there are more complex techniques, such as using splines and wavelets, that in some instances can yield better results than the methods just discussed. While preserving fine detail is an exceptionally important consideration in image generation for 3-D graphics (Watt [1993], Shirley [2002]) and in medical image processing (Lehmann et al. [1999]), the extra computational burden seldom is justifiable for general-purpose digital image processing, where bilinear or bicubic interpolation typically are the methods of choice.

2.5 Some Basic Relationships between Pixels

In this section, we consider several important relationships between pixels in a digital image. As mentioned before, an image is denoted by $f(x, y)$. When referring in this section to a particular pixel, we use lowercase letters, such as p and q.

2.5.1 Neighbors of a Pixel

A pixel p at coordinates (x, y) has four *horizontal* and *vertical* neighbors whose coordinates are given by

$$(x + 1, y), (x - 1, y), (x, y + 1), (x, y - 1)$$

This set of pixels, called the 4-*neighbors* of p, is denoted by $N_4(p)$. Each pixel is a unit distance from (x, y), and some of the neighbor locations of p lie outside the digital image if (x, y) is on the border of the image. We deal with this issue in Chapter 3.

The four *diagonal* neighbors of p have coordinates

$$(x + 1, y + 1), (x + 1, y - 1), (x - 1, y + 1), (x - 1, y - 1)$$

and are denoted by $N_D(p)$. These points, together with the 4-neighbors, are called the 8-*neighbors* of p, denoted by $N_8(p)$. As before, some of the neighbor locations in $N_D(p)$ and $N_8(p)$ fall outside the image if (x, y) is on the border of the image.

2.5.2 Adjacency, Connectivity, Regions, and Boundaries

Let V be the set of intensity values used to define adjacency. In a binary image, $V = \{1\}$ if we are referring to adjacency of pixels with value 1. In a gray-scale image, the idea is the same, but set V typically contains more elements. For example, in the adjacency of pixels with a range of possible intensity values 0 to 255, set V could be any subset of these 256 values. We consider three types of adjacency:

We use the symbols $\cap$ and $\cup$ to denote set intersection and union, respectively. Given sets A and B, recall that their *intersection* is the set of elements that are members of both A and B. The *union* of these two sets is the set of elements that are members of A, of B, or of both. We discuss sets in more detail in Section 2.6.4.

(a) 4-*adjacency*. Two pixels p and q with values from V are 4-adjacent if q is in the set $N_4(p)$.

(b) 8-*adjacency*. Two pixels p and q with values from V are 8-adjacent if q is in the set $N_8(p)$.

(c) *m-adjacency* (mixed adjacency). Two pixels p and q with values from V are m-adjacent if

- **(i)** q is in $N_4(p)$, *or*
- **(ii)** q is in $N_D(p)$ *and* the set $N_4(p) \cap N_4(q)$ has no pixels whose values are from V.

Mixed adjacency is a modification of 8-adjacency. It is introduced to eliminate the ambiguities that often arise when 8-adjacency is used. For example, consider the pixel arrangement shown in Fig. 2.25(a) for $V = \{1\}$. The three pixels at the top of Fig. 2.25(b) show multiple (ambiguous) 8-adjacency, as indicated by the dashed lines. This ambiguity is removed by using *m*-adjacency, as shown in Fig. 2.25(c).

A (*digital*) *path* (or *curve*) from pixel p with coordinates (x, y) to pixel q with coordinates (s, t) is a sequence of distinct pixels with coordinates

$$(x_0, y_0), (x_1, y_1), \ldots, (x_n, y_n)$$

where $(x_0, y_0) = (x, y)$, $(x_n, y_n) = (s, t)$, and pixels (x_i, y_i) and (x_{i-1}, y_{i-1}) are adjacent for $1 \leq i \leq n$. In this case, n is the *length* of the path. If $(x_0, y_0) = (x_n, y_n)$, the path is a *closed* path. We can define 4-, 8-, or *m*-paths depending on the type of adjacency specified. For example, the paths shown in Fig. 2.25(b) between the top right and bottom right points are 8-paths, and the path in Fig. 2.25(c) is an *m*-path.

Let S represent a subset of pixels in an image. Two pixels p and q are said to be *connected* in S if there exists a path between them consisting entirely of pixels in S. For any pixel p in S, the *set* of pixels that are connected to it in S is called a *connected component* of S. If it only has one connected component, then set S is called a *connected set*.

Let R be a subset of pixels in an image. We call R a *region* of the image if R is a connected set. Two regions, R_i and R_j are said to be *adjacent* if their union forms a connected set. Regions that are not adjacent are said to be *disjoint*. We consider 4- and 8-adjacency when referring to regions. For our definition to make sense, the type of adjacency used must be specified. For example, the two regions (of 1s) in Fig. 2.25(d) are adjacent only if 8-adjacency is used (according to the definition in the previous paragraph, a 4-path between the two regions does not exist, so their union is not a connected set).

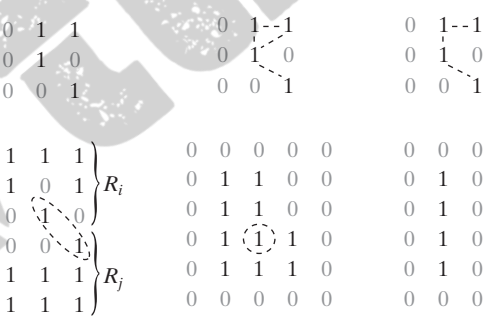

a b c
d e f

FIGURE 2.25 (a) An arrangement of pixels. (b) Pixels that are 8-adjacent (adjacency is shown by dashed lines; note the ambiguity). (c) *m*-adjacency. (d) Two regions (of 1s) that are adjacent if 8-adjecency is used. (e) The circled point is part of the boundary of the 1-valued pixels only if 8-adjacency between the region and background is used. (f) The inner boundary of the 1-valued region does not form a closed path, but its outer boundary does.

Suppose that an image contains K disjoint regions, $R_k, k = 1, 2, \ldots, K$, none of which touches the image border.[†] Let R_u denote the union of all the K regions, and let $(R_u)^c$ denote its complement (recall that the *complement* of a set S is the set of points that are not in S). We call all the points in R_u the *foreground*, and all the points in $(R_u)^c$ the *background* of the image.

The *boundary* (also called the *border* or *contour*) of a region R is the set of points that are adjacent to points in the complement of R. Said another way, the border of a region is the set of pixels in the region that have at least one background neighbor. Here again, we must specify the connectivity being used to define adjacency. For example, the point circled in Fig. 2.25(e) is not a member of the border of the 1-valued region if 4-connectivity is used between the region and its background. As a rule, adjacency between points in a region and its background is defined in terms of 8-connectivity to handle situations like this.

The preceding definition sometimes is referred to as the *inner border* of the region to distinguish it from its *outer border*, which is the corresponding border in the background. This distinction is important in the development of border-following algorithms. Such algorithms usually are formulated to follow the outer boundary in order to guarantee that the result will form a closed path. For instance, the inner border of the 1-valued region in Fig. 2.25(f) is the region itself. This border does not satisfy the definition of a closed path given earlier. On the other hand, the outer border of the region does form a closed path around the region.

If R happens to be an entire image (which we recall is a rectangular set of pixels), then its boundary is defined as the set of pixels in the first and last rows and columns of the image. This extra definition is required because an image has no neighbors beyond its border. Normally, when we refer to a region, we are referring to a subset of an image, and any pixels in the boundary of the region that happen to coincide with the border of the image are included implicitly as part of the region boundary.

The concept of an *edge* is found frequently in discussions dealing with regions and boundaries. There is a key difference between these concepts, however. The boundary of a finite region forms a closed path and is thus a "global" concept. As discussed in detail in Chapter 10, edges are formed from pixels with derivative values that exceed a preset threshold. Thus, the idea of an edge is a "local" concept that is based on a measure of intensity-level discontinuity at a point. It is possible to link edge points into edge segments, and sometimes these segments are linked in such a way that they correspond to boundaries, but this is not always the case. The one exception in which edges and boundaries correspond is in binary images. Depending on the type of connectivity and edge operators used (we discuss these in Chapter 10), the edge extracted from a binary region will be the same as the region boundary.

This is intuitive. Conceptually, until we arrive at Chapter 10, it is helpful to think of edges as intensity discontinuities and boundaries as closed paths.

2.5.3 Distance Measures

For pixels p, q, and z, with coordinates (x, y), (s, t), and (v, w), respectively, D is a *distance function* or *metric* if

(a) $D(p, q) \geq 0 \quad (D(p, q) = 0 \quad \text{iff} \quad p = q)$,
(b) $D(p, q) = D(q, p)$, and
(c) $D(p, z) \leq D(p, q) + D(q, z)$.

The *Euclidean distance* between p and q is defined as

$$D_e(p, q) = \left[(x - s)^2 + (y - t)^2\right]^{\frac{1}{2}} \tag{2.5-1}$$

For this distance measure, the pixels having a distance less than or equal to some value r from (x, y) are the points contained in a disk of radius r centered at (x, y).

The D_4 *distance* (called the *city-block distance*) between p and q is defined as

$$D_4(p, q) = |x - s| + |y - t| \tag{2.5-2}$$

In this case, the pixels having a D_4 distance from (x, y) less than or equal to some value r form a diamond centered at (x, y). For example, the pixels with D_4 distance ≤ 2 from (x, y) (the center point) form the following contours of constant distance:

$$\begin{array}{ccccc} & & 2 & & \\ & 2 & 1 & 2 & \\ 2 & 1 & 0 & 1 & 2 \\ & 2 & 1 & 2 & \\ & & 2 & & \end{array}$$

The pixels with $D_4 = 1$ are the 4-neighbors of (x, y).

The D_8 *distance* (called the *chessboard distance*) between p and q is defined as

$$D_8(p, q) = \max(|x - s|, |y - t|) \tag{2.5-3}$$

In this case, the pixels with D_8 distance from (x, y) less than or equal to some value r form a square centered at (x, y). For example, the pixels with D_8 distance ≤ 2 from (x, y) (the center point) form the following contours of constant distance:

$$\begin{array}{ccccc} 2 & 2 & 2 & 2 & 2 \\ 2 & 1 & 1 & 1 & 2 \\ 2 & 1 & 0 & 1 & 2 \\ 2 & 1 & 1 & 1 & 2 \\ 2 & 2 & 2 & 2 & 2 \end{array}$$

The pixels with $D_8 = 1$ are the 8-neighbors of (x, y).

Note that the D_4 and D_8 distances between p and q are independent of any paths that might exist between the points because these distances involve only the coordinates of the points. If we elect to consider m-adjacency, however, the D_m distance between two points is defined as the shortest m-path between the points. In this case, the distance between two pixels will depend on the values of the pixels along the path, as well as the values of their neighbors. For instance, consider the following arrangement of pixels and assume that p, p_2, and p_4 have value 1 and that p_1 and p_3 can have a value of 0 or 1:

$$\begin{matrix} & p_3 & p_4 \\ p_1 & p_2 & \\ p & & \end{matrix}$$

Suppose that we consider adjacency of pixels valued 1 (i.e., $V = \{1\}$). If p_1 and p_3 are 0, the length of the shortest m-path (the D_m distance) between p and p_4 is 2. If p_1 is 1, then p_2 and p will no longer be m-adjacent (see the definition of m-adjacency) and the length of the shortest m-path becomes 3 (the path goes through the points $pp_1p_2p_4$). Similar comments apply if p_3 is 1 (and p_1 is 0); in this case, the length of the shortest m-path also is 3. Finally, if both p_1 and p_3 are 1, the length of the shortest m-path between p and p_4 is 4. In this case, the path goes through the sequence of points $pp_1p_2p_3p_4$.

2.6.2 Linear versus Nonlinear Operations

One of the most important classifications of an image-processing method is whether it is linear or nonlinear. Consider a general operator, H, that produces an output image, $g(x, y)$, for a given input image, $f(x, y)$:

$$H\big[f(x, y)\big] = g(x, y) \tag{2.6-1}$$

H is said to be a *linear operator* if

$$\begin{aligned} H\big[a_i f_i(x, y) + a_j f_j(x, y)\big] &= a_i H\big[f_i(x, y)\big] + a_j H\big[f_j(x, y)\big] \\ &= a_i g_i(x, y) + a_j g_j(x, y) \end{aligned} \tag{2.6-2}$$

where a_i, a_j, $f_i(x, y)$, and $f_j(x, y)$ are arbitrary constants and images (of the same size), respectively. Equation (2.6-2) indicates that the output of a linear operation due to the sum of two inputs is the same as performing the operation on the inputs individually and then summing the results. In addition, the output of a linear operation to a constant times an input is the same as the output of the operation due to the original input multiplied by that constant. The first property is called the property of *additivity* and the second is called the property of *homogeneity*.

As a simple example, suppose that H is the sum operator, Σ; that is, the function of this operator is simply to sum its inputs. To test for linearity, we start with the left side of Eq. (2.6-2) and attempt to prove that it is equal to the right side:

$$\begin{aligned} \sum\big[a_i f_i(x, y) + a_j f_j(x, y)\big] &= \sum a_i f_i(x, y) + \sum a_j f_j(x, y) \\ &= a_i \sum f_i(x, y) + a_j \sum f_j(x, y) \\ &= a_i g_i(x, y) + a_j g_j(x, y) \end{aligned}$$

These are array summations, not the sums of all the elements of the images. As such, the sum of a single image is the image itself.

where the first step follows from the fact that summation is distributive. So, an expansion of the left side is equal to the right side of Eq. (2.6-2), and we conclude that the sum operator is linear.

On the other hand, consider the max operation, whose function is to find the maximum value of the pixels in an image. For our purposes here, the simplest way to prove that this operator is nonlinear, is to find an example that fails the test in Eq. (2.6-2). Consider the following two images

$$f_1 = \begin{bmatrix} 0 & 2 \\ 2 & 3 \end{bmatrix} \quad \text{and} \quad f_2 = \begin{bmatrix} 6 & 5 \\ 4 & 7 \end{bmatrix}$$

and suppose that we let $a_1 = 1$ and $a_2 = -1$. To test for linearity, we again start with the left side of Eq. (2.6-2):

$$\max\left\{(1)\begin{bmatrix} 0 & 2 \\ 2 & 3 \end{bmatrix} + (-1)\begin{bmatrix} 6 & 5 \\ 4 & 7 \end{bmatrix}\right\} = \max\left\{\begin{bmatrix} -6 & -3 \\ -2 & -4 \end{bmatrix}\right\}$$
$$= -2$$

Working next with the right side, we obtain

$$(1)\max\left\{\begin{bmatrix} 0 & 2 \\ 2 & 3 \end{bmatrix}\right\} + (-1)\max\left\{\begin{bmatrix} 6 & 5 \\ 4 & 7 \end{bmatrix}\right\} = 3 + (-1)7$$
$$= -4$$

The left and right sides of Eq. (2.6-2) are not equal in this case, so we have proved that in general the max operator is nonlinear.

As you will see in the next three chapters, especially in Chapters 4 and 5, linear operations are exceptionally important because they are based on a large body of theoretical and practical results that are applicable to image processing. Nonlinear systems are not nearly as well understood, so their scope of application is more limited. However, you will encounter in the following chapters several nonlinear image processing operations whose performance far exceeds what is achievable by their linear counterparts.